Impact of changes in proximal tubular reabsorption on kidney function and on blood flow synchronization among nephrons

by

Shayan Poursharif

A thesis submitted in partial fulfillment of the requirements for the degree of

Master of Science

Department of Medicine

University of Alberta

Abstract

Kidneys stabilize renal blood flow (RBF) in response to fluctuations in blood pressure by employing two mechanisms, the myogenic response (MR) and the tubuloglomerular feedback (TGF) mechanism. The TGF mechanism stabilizes macula densa solute delivery via controlling afferent arteriolar diameter. Furthermore, TGF generates oscillations within each nephrovascular unit (NVU), each nephron and its afferent and efferent arteriole, and oscillatory systems with similar frequencies can entrain and become synchronized.

SGLT2 inhibitors can improve renal function in the early and advanced diabetic nephropathy by increasing macula densa solute delivery, activating the TGF mechanism and presumably improving synchronization among NVUs. Consequently, enhancing synchronization among NVUs by activating the TGF mechanism might improve renal hemodynamics and preserve renal function in diabetic nephropathy and non-diabetic chronic kidney disease (CKD). This is prominent as more than 3 million Canadians are suffering from CKD [1], which puts a great financial burden on the health care system. We used different compounds that could change TGF activity to understand synchronization among NVUs better and to see how the synchronization among NVUs would be affected.

In our first aim, we tried to inhibit the sensing step of the TGF mechanism by administering high dose furosemide to assess synchronization among nearby NVUs in male Lewis rats (n=8). We hypothesized that inhibiting the TGF mechanism by administrating high dose furosemide would weaken synchronization among nearby NVUs.

In our second and third aim, we tested the effects of activating the TGF mechanism on synchronization among nearby NVUs, by administrating acetazolamide (n=6) and low dose furosemide (n=6) in male Lewis rats. We hypothesized that administrating acetazolamide and low dose furosemide enhance synchronization among nearby NVUs by activating TGF.

In all the experiments, laser speckle contrast imaging (LSI), which can probe surface renal perfusion, was used to assess TGF phase coherence (PC), the number of edges with PC > 0.6, the magnitude of decay of TGF_{PC} and the initial and secondary decay associated with TGF_{PC}. These parameters can be used to assess strength of synchronization among NVUs.

Our results illustrate that high dose furosemide did not change PC and the number of edges with PC > 0.6, indicating no changes in synchronization among nearby NVUs. Interestingly, high dose furosemide decreased the magnitude of decay of TGF_{PC} showing stronger synchronization among NVUs. The inconsistency in these findings suggests the complexity of high dose furosemide as it causes vasodilation, increases macula densa solute delivery, changes TGF responsiveness and affects renin and ANG II levels. Moreover, technical issues could be another explanation for inconsistent findings as movements of the kidney surface due to pulse or/and respiration could be also captured by the LSI, which would affect the number of edges and PC.

Additionally, acetazolamide and low dose furosemide increased mean PC, the number of edges with PC > 0.6 and decreased the magnitude of decay of TGF_{PC}, indicating stronger synchronization among nearby NVUs. It can be concluded from these findings that synchronization among NVUs can be enhanced by activating the TGF mechanism.

Preface

This thesis project is done by Shayan Poursharif. The research conducted for this thesis was done with technical support from Dr. Branko Braam, Dr. Shereen Hamza and Wenqing Zhuang who provided tremendous support during the experiments. Dr. Branko Braam, Dr William A. Cupples, Dr. Heather More and Tayyaba Zehra helped with the data analysis codes, explained in methodology, which were used to analyze and interpret the data. Dr. Branko Braam, Dr. William A. Cupples and Dr. Shereen Hamza were the supervisory committees and helped tremendously with forming the concept and manuscript revision. I was accountable for data collection, analysis, and writing the manuscript.

The literature review in chapter 2 has been published as Poursharif S, Hamza S, Braam B. Changes in Proximal Tubular Reabsorption Modulate Microvascular Regulation via the TGF System. Int J Mol Sci. 2022 Sep 23;23(19):11203. doi: 10.3390/ijms231911203. PMID: 36232506; PMCID: PMC9569689. All chapters of this thesis are my original work.

Acknowledgements

I would like to acknowledge and give my deepest thanks to my supervisor and guide Dr. Branko Braam for his tremendous support, guidance, motivation, and enthusiasm through my studies. He mentored me in every step of the way during my studies to become a better researcher, physician, and person. I would also like to warmly thank my other supervisors and mentors, Dr. William A. Cupples and Dr. Shereen Hamza for their patience, supports, guidance and brilliants comments and suggestions throughout my studies.

I would like to acknowledge Tayyaba Zehra and Wenqinq Zhuang for their supports and helps during the projects. I am also grateful to Dr. Heather More for her supports with analysing the data.

Finally, I would like to thank the Department of Medicine, University of Alberta, for the opportunity to pursue my passion in nephrology.

Table of Contents

List of Tables

List of Figures

List of Abbreviations

A	Magnitude of decay of tubuloglomerular feedback phase coherence
ACEi	Angiotensin converting enzyme inhibitor
ANG II	Angiotensin II
ANP	Atrial natriuretic peptide
ARB	Angiotensin II receptor blocker
ATP	Adenosine Triphosphate
BSA	Bovine serum albumin
cAMP	Cyclic adenosine monophosphate
cGMP	Cyclic guanosine monophosphate
CCB	Calcium channel blocker
Cl	Chlorine
CKD	Chronic kidney disease
FITC	Fluorescein isothiocyanate
GFR	Glomerular filtration rate
HNF-1a	Hepatocyte nuclear factor
HR	Heart rate
IL-6	Interleukin 6
K	Potassium
K_1	Initial decay associated with TGF phase coherence
K_2	Secondary decay associated with TGF phase coherence
LiCl	Lithium chloride
LSI	Laser spackle contrast imaging

MAP	Mean arterial pressure
MR	Myogenic response
Na	Sodium
NaCl	Sodium-chloride
NHE	Sodium-hydrogen exchanger
NHE1	Sodium-hydrogen exchanger 1
NHE2	Sodium-hydrogen exchanger 2
NHE3	Sodium-hydrogen exchanger 3
NKCC2	Na-K-2Cl co-transporter
NO	Nitric oxide
NVU	Nephrovascular unit
PC	Phase coherence
PGC	Glomerular capillary pressure
PGE2	Prostaglandin E2
PTH	Parathyroid hormone
RAS	Renin-angiotensin system
RBF	Renal blood flow
ROS	Reactive oxygen species
RVR	Renal vascular resistance
SGLT	Sodium glucose co-transporter
TAL	Thick ascending limb of loop of Henle
TGF	Tubuloglomerular feedback

Chapter 1: Introduction

Background

Kidneys stabilize renal blood flow (RBF) and glomerular filtration rate (GFR) in response to alterations in blood pressure to prevent glomeruli injury [2]. This is achieved by two mechanisms, the rapid myogenic response (MR) and the slower tubuloglomerular feedback (TGF) mechanism. MR is a universal mechanism, a rapid constriction of vessels in response to an increase in wall tension induced by surges in blood pressure. In the kidneys, this implies that an increase in renal arterial pressure (RAP) leads to a reduction in afferent arteriolar diameter and increased renal perivascular resistance which prevents an increase of RBF and GFR. The TGF mechanism stabilizes macula densa solute delivery via controlling afferent arteriolar diameter. Increase in RBF and GFR eventually leads to an increase in solute concentration of fluid reaching macula densa. This is sensed by Na-K-2Cl cotransporter (NKCC2) at macula densa and results in release of adenosine and ATP, which will constrict afferent arteriole. Consequently, GFR and RBF return to baseline which would eventually reduce solute concentration of fluid reaching macula densa [3].

The notion that each nephron is accountable for its own autoregulation has changed due to complex nature of renovascular physiology and anatomy. Nephrovascular units (NVUs) (nephrons with attached afferent and efferent arterioles) form a network in autoregulation of RBF and explain renal blood flow autoregulation and perfusion in the kidneys better [4]. This is mediated by TGF. TGF produces oscillations within each NVU and oscillatory systems with similar frequencies can entrain and become coupled (synchronized) [5-7]. This coupling among NVUs could prevent a discrepancy between oxygen demand and delivery as each NVU's tubule is perfused by 4-5 nearby NVUs, which increases RBF autoregulation efficacy [4].

Laser speckle contrast imaging (LSI), which probes renal cortical perfusion, can be used to assess TGF-mediated nephron synchronization and network among NVUs. Previous studies using LSI showed that carbenoxolone, a gap junction inhibitor, impairs TGF synchronization and renal blood flow autoregulation [8]. However, compounds that can enhance or weaken TGF synchronization among NVUs have not been studied thoroughly.

Important proximal tubular and loop of Henle sodium transporters are sodium-hydrogen exchanger 3 (NHE3), NKCC2 and sodium-glucose co transporter 2 (SGLT2). Acetazolamide, furosemide and SGLT2 inhibitors are the most important compounds that can inhibit these transporters and decrease proximal tubular/loop of Henle sodium reabsorption. Consequently, they can increase solute concentration of fluid reaching macula densa, activate the TGF and might strengthen the network among NVUs. Enhancing synchronization among nephrons may lead to enhancing kidney function in early and advanced diabetic nephropathy and non-diabetic CKD.

Objectives of thesis

In the first aim, we examined the effects of inhibiting the TGF mechanism on synchronization among nearby NVUs. Furosemide (Lasix) decreases solute reabsorption proximal to macula densa by inhibiting the NKCC2 transporters in the loop of Henle. This can increase solute concentration of fluid reaching macula densa. However, furosemide can (partially) inhibit the sensing step of the TGF mechanism by inhibiting NKCC2 in the macula densa. This would make the TGF mechanism ineffective, which might decrease synchronization (coupling) among NVUs. It is suggested that higher tubular concentration of furosemide is needed to inhibit the sensing step of TGF responses [9]. We hypothesized that inhibiting TGF response by higher dose of furosemide (10, 20, 30 mg/kg) decreases synchronization among nearby NVUs.

In the second aim, we examined the effects of activating the TGF mechanism on synchronization among nearby NVUs by acetazolamide. Acetazolamide, which is a carbonic anhydrase inhibitor, decreases proximal tubular solute reabsorption by decreasing carbonic anhydrase activity and NHE3 function in the proximal tubule. This can increase solute concentration of fluid reaching macula densa and activate TGF mechanism. We hypothesized that activating the TGF response by acetazolamide enhances synchronization among nearby NVUs.

In the third aim, we examined the effects of activating the TGF mechanism on synchronization among nearby NVUs. Low dose furosemide (1 mg/kg) decreases solute reabsorption in the loop of Henle by inhibiting the NKCC2 transporters. This can increase solute concentration of fluid reaching macula densa and activate the TGF. As extremely high tubular concentration of furosemide is needed to inhibit NKCC2 transporters in macula densa, we hypothesized that

administration of low dose furosemide does not inhibit the TGF mechanism and enhances synchronization among nearby NVUs by activating it.

Chapter 2: Literature review

Abstract

This review paper considers the consequences of modulating tubular reabsorption proximal to the macula densa by sodium–glucose co-transporter 2 (SGLT2) inhibitors, acetazolamide, and furosemide in states of glomerular hyperfiltration. SGLT2 inhibitors improve renal function in early and advanced diabetic nephropathy by decreasing the glomerular filtration rate (GFR), presumably by activating the tubuloglomerular feedback (TGF) mechanism. Central in this paper is that the renoprotective effects of SGLT2 inhibitors in diabetic nephropathy can only be partially explained by TGF activation, and there are alternative explanations. The sustained activation of TGF leans on two prerequisites: no or only partial adaptation should occur in reabsorption proximal to macula densa, and no or only partial adaptation should occur in the TGF response. The main proximal tubular and loop of Henle sodium transporters are sodium–hydrogen exchanger 3 (NHE3), SGLT2, and the Na-K-2Cl co-transporter (NKCC2). SGLT2 inhibitors, acetazolamide, and furosemide are the most important compounds; inhibiting these transporters would decrease sodium reabsorption upstream of the macula densa and increase TGF activity. This could directly or indirectly affect TGF responsiveness, which could oppose sustained TGF activation. Only SGLT2 inhibitors can sustainably activate the TGF as there is only partial compensation in tubular reabsorption and TGF response. SGLT2 inhibitors have been shown to preserve GFR in both early and advanced diabetic nephropathy. Other than for early diabetic nephropathy, a solid physiological basis for these effects in advanced nephropathy is lacking. In addition, TGF has hardly been studied in humans, and therefore this role of TGF remains elusive. This review also considers alternative explanations for the renoprotective effects of SGLT2 inhibitors in diabetic patients such as the enhancement of microvascular network function. Furthermore, combination use of SGLT2 inhibitors and angiotensin-converting enzyme inhibitors (ACEi) or angiotensin

receptor blockers (ARBs). in diabetes can decrease inflammatory pathways, improve renal oxygenation, and delay the progression of diabetic nephropathy.

Introduction

Recent studies strongly support that sodium-glucose co-transporter type 2 (SGLT2) inhibitors decrease cardiovascular risk [10, 11]. In addition, these drugs preserve renal function, presumably by enhancing tubuloglomerular feedback (TGF) [12-15]. In this paper, we challenge this assumption. There is a widespread belief that SGLT2 inhibition causes a sustained increase in macula densa delivery leading to a sustained activation of TGF which then would sustainably lower glomerular capillary pressure (PGC). However, there are two prerequisites for this proposition. First, adaptations in reabsorption upstream of the macula densa should not offset the original change in reabsorption. Second, no compensation should occur in the TGF mechanism that could offset a sustained TGF response. In this review, we extend our focus beyond SGLT2 inhibitors and consider several substances and conditions regarding these two prerequisites to help elucidate how these drugs may confer cardiovascular protection in situations where there is hyperfiltering states such as CKD.

SGLT2 inhibitor, acetazolamide and furosemide are compounds that can increase macula densa delivery and activate the TGF response and possibly can decrease hyperfiltration. However, SGLT2 inhibitors seem to be the prototype of drugs to increase macula densa solute delivery and activate TGF response sustainably without changing TGF responsiveness. In contrast, furosemide and acetazolamide have characteristics that possibly fail to meet the prerequisites and prevent sustained increases in TGF activation. Besides the effect of single drugs, we will explore the effect of SGLT2 inhibitors in the real-life context of multiple medications for the treatment of diabetes

mellitus and cardiovascular disease. An example would be the combined use SGLT2 inhibitors and angiotensin-converting enzyme inhibitors (ACEi) or angiotensin receptor blockers (ARBs). These latter drugs would supposedly decrease TGF responsiveness, yet the large clinical trials showing the beneficial effects of SGLT2 inhibitors on renal function were performed in study populations where ACEi and ARB use was highly prevalent [16].

Another aspect of this is, that while SGLT2 inhibitors originally were reported to specifically diminish diabetic hyperfiltration of early diabetic nephropathy before anatomical injury to the glomerulus, they also exert preventative properties in more advanced diabetic nephropathy with segmental or global glomerulosclerosis. We will review proximal tubular reabsorption and TGF dynamics in early versus more advanced diabetic nephropathy. Taken together, given what we know about SGLT2 inhibitors, TGF activation might be a component of the beneficial renal effects of SGLT2 inhibitors in diabetic nephropathy, but other mechanisms are likely and will be discussed.

Autoregulation

Kidneys stabilize RBF (renal blood flow), GFR and PGC in parallel in response to fluctuations in blood pressure by adjustments in afferent arteriolar resistance, by employing two mechanisms, the rapid myogenic response (MR) and the slower TGF. This autoregulation process stabilizes renal function and protects the glomeruli from injury [2]. This is depicted in Figure 1.

MR is a universal response in all microvascular beds: a rise in wall tension, generally due to an increase in blood pressure, results in arteriolar vasoconstriction to stabilize tissue perfusion [17-

22]. In the kidneys, transmission of an increase in arterial pressure to the renal microvasculature leads to afferent arteriolar vasoconstriction, increased renal preglomerular resistance and stabilization of RBF, PGC and GFR [2, 22]. Calcium channel blockers can impair MR and decrease the gain of RBF autoregulation [19, 23]. TGF is the second mechanism participating in RBF autoregulation [2, 17, 18, 24]. Any residual increase in PGC and single nephron GFR (SNGFR) after compensation by MR will lead to an increase in filtered load. Although a higher filtered load increases solute reabsorption in proximal tubule and loop of Henle (glomerulotubular balance) [25], this still leads to an increase in solute delivery to the macula densa. This is sensed by the macula densa and results in release of adenosine and ATP, which will lead to constriction of the afferent arteriole of the same nephron. This, in turn, reduces single nephron GFR and RBF back to baseline, and eventually stabilizes solute delivery to the macula densa [3, 21, 26, 27]. Inhibiting TGF reduces RBF autoregulation efficacy but does not abolish it [2, 3]. TGF saturation is defined as the macula densa delivery, where any further increase would not result in any further activation of TGF and consequently further decrease in SNGFR. Full TGF deactivation is defined as the macula densa delivery at which there is no influence of TGF on SNGFR. TGF responsiveness is defined as the maximum decrease in SNGFR elicited by full activation of TGF. A sustained TGF response means that the depression of SNGFR by TGF activation upon a change in macula densa delivery remains the same over time. TGF blockade is the situation where a high concentration of furosemide is fully blocking how the macula densa can sense sodium, which is via the NKCC2 channel.

MR and TGF interact synergistically [22, 28]. It was demonstrated that with the influence of TGF, the afferent arteriole has a lower diameter and a further decrease in afferent arteriole diameter due

to MR is markedly enhanced [22, 25, 28]. MR in combination with TGF is needed for an optimal RBF autoregulation and MR with its higher frequency acts as a dampening system, whereas TGF with its lower frequency modulates MR and represents fine-tuning stabilization of renal function [29].

As mentioned in the introduction, compounds that decrease solute reabsorption upstream of the macula densa can sustainably increase macula densa delivery. However, partial compensation in reabsorption in segments proximal to the macula densa or resetting or saturation of the TGF system could offset this initial response. The overall thought is depicted in Figure 2.

Tubular reabsorption proximal to macula densa

Reabsorption of sodium together with other solutes like glucose, amino acids, chloride and bicarbonate in the proximal tubule and loop of Henle ultimately determines the solute concentrations of fluid reaching macula densa and the activation of TGF. In this section, we will further discuss the main sodium transporters in this context, NHE3, SGLT2 and the Na-K-2Cl co-transporter, NKCC2, and how they are regulated.

The three isoforms of the sodium-hydrogen exchanger (NHE1, NHE2 and NHE3) in the proximal tubule and descending and ascending loop of Henle [30, 31] are mainly responsible for reabsorption of sodium and bicarbonate. In a series of micropuncture studies in male Wistar rats, luminal amiloride, which inhibits NHE, significantly decreased NaCl and bicarbonate reabsorption in the proximal tubule [32, 33]. Of the NHEs, inhibition of NHE3 in superficial nephrons of

anesthetized rats reduced sodium and fluid reabsorption markedly [34]. Consequently, it is suggested that NHE3 is responsible for reabsorption of a substantial proportion of sodium and bicarbonate in S1 and S2 segments of the proximal tubule, with concomitant paracellular water and chloride reabsorption [14].

NHE3 is regulated by several stimulatory and inhibitory hormones at transcriptional and post-translational levels including changes in protein phosphorylation and trafficking [35]. Insulin and glucocorticoids increased NHE3 activity by increasing NHE3 transcription in opossum kidney cells [36, 37]. PTH decreased NHE3 activity in opossum kidney cells by phosphorylating NHE3 at various serine sites and decreasing surface NHE3 [38]. Angiotensin II (ANG II) increased NHE3 function by changing NHE3 phosphorylation [39-41]. In addition, it has been demonstrated that NHE3 and SGLT2 interact functionally in the proximal tubule as inhibition of SGLT activity in rats by both empagliflozin and phlorizin significantly decreased NHE3 activity [42, 43]. As such, compounds and hormones that directly or indirectly affect NHE3 regulation and activity can markedly affect solute concentration of fluid reaching macula densa and might affect other transporters.

Under physiological conditions, the sodium-glucose co-transporters (SGLTs) SGLT1 and SGLT2 in the proximal tubule reabsorb almost all the filtered glucose [14]. This is achieved by the low-affinity/high-capacity SGLT2 in the early proximal tubule and the high-affinity/low-capacity SGLT1 in the late proximal tubule [15, 44]. SGLT2 reabsorbs sodium and glucose on a 1:1 ratio, while SGLT1 reabsorbs two sodium ions along with one glucose molecule [45]. Moreover, like

NHE3, SGLT2 participates in paracellular Cl and water reabsorption by creating an osmotic gradient [14] .

SGLT2 is upregulated at the transcriptional and post-translational level by ANG II, insulin, and hepatocyte nuclear factor (HNF-alpha) [46, 47]. Increased transcription of the transcription factor HNF-1 alpha in diabetic rats was associated with increased binding of HNF-1 into the SGLT2 promoter region which then likely caused increased SGLT2 expression [48]. Additionally, phosphorylation of SGLT2 by activating protein kinase A and C in human embryonic kidney 293T cells increased reabsorption of sodium and glucose markedly [49].

In the loop of Henle, 25-30% of filtered Na-Cl is reabsorbed via NKCC2 across the apical membrane of the water impermeable thick ascending limb (TAL) [50, 51]. Ninety percent of reabsorbed potassium via NKCC2 is secreted back into the lumen through inward rectifying K channels in the apical membrane. Secretion of potassium to lumen and absorption of chloride from the basolateral membrane to the circulation via chloride channels generates a lumen-positive transepithelial potential difference. This mediates paracellular reabsorption of sodium, magnesium, and calcium [51-53]. Unlike TAL, the thin limb of Henle generally has low permeability to sodium and does not contribute significantly to sodium reabsorption [54-56].

Several hormones modulate NaCl reabsorption in TAL by regulating NKCC2 activity. NKCC2 is stimulated at the post-translational level mainly via increasing intracellular cAMP levels by stimulatory hormones such as vasopressin, PTH and calcitonin. cAMP enhances NKCC2 activity by stimulating insertion of them into the cell membrane and presumably also by phosphorylation

[50]. Stimulation of NKCC2 by phosphorylation was shown in cultured TAL cells from rabbits and in rats with diabetes insipidus after administrating vasopressin agonists [57]. Conversely, NO, atrial natriuretic peptides (ANP), endothelin, prostaglandin E2 (PGE2) inhibit NKCC2 mainly via cGMP by decreasing its trafficking [50, 51]. It was also shown that Ang II increased NaCl transport in rats TAL by blunting NO induced inhibition of NKCC2, which increased NKCC2 activity [58, 59]. Furthermore, administration of indomethacin and diclofenac, prostaglandin inhibitors, in rats increased solute reabsorption in loop of Henle by upregulating NKCC2, while misoprostol, a PGE2 analog, reset this effect [60]. From the above it is clear that NKCC2 activity is modulated by many factors.

Effects of early and advanced diabetes on macula densa solute delivery and the TGF response

In the early phase of diabetic nephropathy, proximal tubular reabsorption is increased, resulting in decreased solute delivery to the macula densa and deactivation of the TGF response [61], hyperfiltration and progression of glomerular damage. This in turn could change solute reabsorption upstream of the macula densa and alter the TGF response in a variety of ways. We will discuss how macula densa solute delivery and the TGF system are affected in early and advanced diabetic nephropathy.

In diabetes mellitus, the filtered load of glucose is increased. Nephrons become hypertrophied and SGLT2 expression increases in the proximal tubule [15]. Increased reabsorption by SGLT2s would result in decreased solute concentration of fluid reaching macula densa, deactivation of TGF (unloading macula densa transporters) and hyperfiltration. That the hyperfiltration was a response

to increased transport by SGLT2 was shown in streptozotocin induced type 2 diabetic mice and Akita mouse models of type 1 diabetes: hyperfiltration did not occur if diabetes was induced in SGLT2 knockout mice [62]. Additionally, in early diabetes, the turning point of the TGF curve can be shifted upward (TGF is reset upward) which can exacerbate the hyperfiltration [63]. Furthermore, plasma and kidney ANG II levels are increased in diabetes mellitus [64]. This was also shown in several type 1 and type 2 animal models as derived from increased angiotensinogen levels [65-67]. Increased ANG II levels in diabetes can modulate the TGF system in several ways. As mentioned, ANG II enhances solute reabsorption in the proximal tubule and loop of Henle. Therefore, macula densa solute delivery decreases and TGF is deactivated, which could exacerbate hyperfiltration [68, 69]. However, ANG II resets the turning point of the TGF curve to a lower level, so that potentially SNGFR does not change in response to increased ANG II [70]. Taken together, in early diabetic nephropathy, increased solute reabsorption by SGLT2s would result in hyperfiltration, while increased ANG II might exacerbate hyperfiltration slightly.

In advanced diabetic nephropathy, nephrons can display at least three different phenotypes: intact nephrons, segmentally sclerosed nephrons and globally sclerosed nephrons. The intact, often hypertrophied nephrons might display enhanced reabsorption due to the same mechanisms as in early diabetes. Increased ANG II levels and increased activity of SGLT2 transporters will contribute to deactivation of the TGF and cause hyperfiltration.

Additionally, some nephrons can become segmentally sclerosed, which can result in decreased filtration, decreased macula densa delivery and deactivation of TGF. In these partially sclerosed

nephrons GFR might or might not be increased based on the extent of glomerular sclerosis. If there is an adequate glomerular surface, GFR would increase. Otherwise, GFR would remain low.

Finally, some nephrons are globally sclerosed and there is no filtration and TGF activity. This would contribute to an overall decrease in GFR. These globally sclerosed nephrons no longer consume oxygen. As further explained below, such nephrons can also disturb microvascular network dynamics in two ways. First, they can cause anatomical disruption. Second, they disrupt oxygenation of nearby intact nephrons, which can result in decreased solute reabsorption, increased macula densa solute delivery, activation of TGF and decrease SNGFR in nearby intact nephrons.

Additionally, volume expansion in advanced diabetic nephropathy might affect macula densa delivery and the TGF system. Volume expansion decreases ANGII levels [71]. This would lead to decreased reabsorption and TGF responsiveness [72] in the intact and partially sclerosed nephrons, which would result in decreased GFR.

In summary, in early diabetic nephropathy solute concentration of fluid reaching macula densa decreases and TGF is deactivated, which would result in hyperfiltration. In advanced diabetic nephropathy the changes in reabsorption and the TGF response are difficult to predict due to segmental or global glomerulosclerosis and potential volume expansion (Figure 3).

Effects of SGLT2 inhibitors on macula densa delivery and TGF response

Clinically, SGLT2 inhibitors are effective in reducing cardiovascular events and in preventing CKD progression in mild, but also more advanced diabetic as well as non-diabetic CKD [10, 11, 73]. SGLT2 inhibitors directly and indirectly (via NHE3) inhibit reabsorption of sodium in the proximal tubule, resulting in an immediate increase in solute delivery to the macula densa [43, 54]. Chronically, this is partially offset by an increase in the function of SGLT1 in the proximal tubule as well as an increase in loop of Henle solute reabsorption [13]. In a series of micropuncture studies assessing acute and chronic effects of the SGLT2 inhibitor, dapagliflozin, on proximal tubular reabsorption in streptozotocin induces diabetic rats, it was concluded that the inhibitory effect of dapagliflozin on proximal reabsorption is partially compensated by increase in loop of Henle solute reabsorption [13]. Also, inhibition of SGLT2 in mice showed an increase in glucose reabsorption by SGLT1 from 3% to 50-60% of total glucose reabsorption [74]. Besides this, the turning point of TGF curve can be shifted during chronic SGLT2 inhibition. An increase in solute concentration of fluid reaching macula densa in mouse renal cortex can lead to generation of nitric oxide [75]. This has been shown to offset the TGF response in mice and rats [76-78].

Nevertheless, SGLT2 inhibitors can sustainably increase solute concentration of fluid reaching macula densa, and lead to a sustained TGF activation, afferent arteriolar vasoconstriction and decline in SNGFR and whole kidney GFR. However, in the only available study on this subject, the sustained response was 50% of the acute response [13-15].

Besides different phases of diabetic and non-diabetic CKD, an area of great uncertainty is whether other concomitant treatments could offset the beneficial effects of SGLT2 inhibitors. An example

is ACE inhibitor therapy. It has been documented by us [79, 80] and others [81-83] that acute administration of ACE inhibitors decreases the TGF maximum response as well as increases the tubular fluid flow exerting a half-maximum TGF response in experimental animals. Nevertheless, we are only aware of one study from our own group demonstrating that after prolonged ACE inhibition, the TGF response returns [84]. Whether during prolonged ACE inhibition a TGF response is present and of normal magnitude in humans is entirely unknown. Similar considerations would apply to intensive treatment with calcium channel blockers and loop diuretics: these medications could also modify TGF responsiveness and modulate the response to SGLT2 inhibition, but information in both experimental settings and in humans is lacking.

The available literature about the mechanistic aspects of the positive effects of SGLT2 inhibitors in early diabetic nephropathy is based on a relatively small number of studies in rats and mice supporting the idea that these compounds increase solute concentration of fluid reaching macula densa sustainably and activate TGF sustainably which reduce hyperfiltration and thereby preserve renal function. The literature is lacking a solid basis for how SGLT2 inhibitors exert their actions in more advanced diabetic and non-diabetic CKD. In addition, TGF is difficult to assess and has hardly been studied in humans and whether TGF is the central mediator of positive effects of SGLT2 inhibitors in human diabetic and non-diabetic CKD patients remains elusive.

Effects of ACTZ on macula densa delivery and TGF response

Acetazolamide reduces proximal tubular reabsorption by inhibiting bicarbonate reabsorption via decreasing carbonic anhydrase activity and NHE3 [85]. This initially increases macula densa solute delivery. Despite a compensatory increase in proximal tubular and loop of Henle solute

reabsorption due to increase in ANG II levels [86], acetazolamide can increase the solute concentration of fluid reaching macula densa sustainably and initially reduces GFR by activating TGF and potentially increasing proximal tubular pressure [87, 88]. However, TGF does not remain activated due to upward and rightward resetting of the turning point of the TGF curve, possibly due to increased NO levels [89-91]. In a study assessing autoregulation, increased renal glomerular pressure resulted in an immediate afferent arteriolar vasoconstriction followed by a moderate decline of afferent arteriolar vasoconstriction (sustained response). Acetazolamide administration enhanced the initial vasoconstriction, but it did not alter the sustained response. Inhibition of NO enhanced both initial and sustained constrictor response to acetazolamide [92]. Consequently, acetazolamide did not sustainably change single nephron and whole kidney hemodynamics due to compensation occurring in the TGF response (TGF resetting). Of note, acetazolamide would have been an interesting control in studies about SGLT2 inhibitors since it sustainably decreases proximal tubular reabsorption but does not sustainably activate TGF, and both compounds are diuretics.

Effects of furosemide on macula densa delivery and TGF response

Furosemide reduces sodium reabsorption in the thick ascending limb of loop of Henle by inhibiting NKCC2, which would initially increase the solute concentration of fluid reaching macula densa. While this can be compensated by increasing solute reabsorption in the proximal tubule due to activation of RAS and sympathetic nervous system, furosemide can increase solute concentration of fluid reaching macula densa sustainably [9]. That said, the effect of furosemide on the TGF system are less clear. One scenario is that furosemide would activate and then saturate the TGF response, effectively eliminating TGF dynamics on renal autoregulation. Another option is that

furosemide can (partially) inhibit the sensing step of the TGF system since this is formed by NKCC2 in the macula densa. This would also prevent a sustained activation of the TGF response. It is suggested that tubular concentration of furosemide is the determinant of the balance between these two opposite responses [9]. Consequently, while furosemide can sustainably increase solute concentration of fluid reaching macula densa, it is not clear whether it can sustainably alter TGF activation.

Alternative explanations for the beneficial effects of SGLT2 inhibitors in CKD

Although the data in the literature is sparse, there are other explanations for the positive effects of SGLT2 inhibitors in diabetic nephropathy. SGLT2 inhibitors could enhance network function among nephrons by activating the TGF system. In addition, combination use of SGLT2 inhibitors and ARBs/ACEi can reduce fibrosis, inflammatory pathways and glomerular injury in diabetes and thereby preserve renal function. Furthermore, SGLT2 inhibitors and ARBs/ACEi decrease tubular reabsorption. This reduces oxygen demand and renal hypoxia, which are known cause of fibrosis and microvascular injury [93].

Recognition of the complexity of kidney's microvascular physiology and anatomy has altered the idea that each nephron is responsible for its own autoregulation. We and others have suggested that nephrovascular units (NVUs), which consist of a nephron and its afferent and efferent arteriole, communicate with each other in a network, and explain renal autoregulation and perfusion in the kidneys better [4]. TGF generates oscillations within each NVU and oscillatory systems with similar frequencies can entrain and become synchronized [5-7]. This synchronization among NVUs, which increases RBF autoregulation efficacy, could prevent a

discrepancy between metabolic demand and oxygen delivery as each NVU's tubule is perfused by 4-5 nearby NVUs [4]. Consequently, one theory explaining the renoprotective effects of SGLT2 inhibitors is that they can enhance network dynamics among NVUs activate the TGF response sustainably.

Moreover, TGF generated oscillations can be transmitted to upstream vascular branch points through endothelial gap junctions formed by connexin proteins (mainly connexin 40) [4]. This upstream "electrical cable" enables communication between NVUs at vascular branch points and optimizes network among them. It was shown that treating mice with the metabolic syndrome with SGLT2 inhibitors, prevented the decline in connexin 40 in these animals [94]. Consequently, SGLT2 inhibitors can also directly affect the transmission of TGF oscillations to upstream microvasculature and thereby enhance network function amongst them.

Another explanation for the beneficial effects of SGLT2 inhibitors could be the combined use of SGLT2 inhibitors and ACEi or ARBs in diabetic patients. Increased luminal glucose by SGLT2 inhibitors inhibits urate transporter 1, which would increase uric acid excretion substantially. This in turn would reduce ROS, inflammation, and renal damage induced by uric acid [76]. SGLT2 inhibitors can also reduce mRNA expression of proinflammatory mediators such as nuclear factor-KB and IL-6 levels in the kidney [95] [96]. Moreover, it was shown that ACEi can prevent tubulointerstitial fibrosis, tubular apoptosis and renal oxidative stress in animal studies [97, 98]. Furthermore, combined use of SGLT2 inhibitors and ACE inhibitors reduces tubular reabsorption additively, which can further decrease hyperfilterarion. Moreover, this reduces oxygen demand and would improve renal oxygen levels [93]. Consequently, combination of SGLT2 inhibitors and

ARBs/ACEi could have synergistic effects to decrease inflammatory pathways, improve renal oxygenation and delay progression of diabetic nephropathy. Nevertheless, ambiguity remains about the combination of SGLT2 and ARBs/ACEi since acute administration of ARBs/ACEi decrease TGF responsiveness in rats and thereby could attenuate the TGF activation by SGLT2 inhibitors [84]. There is no data available about TGF responses in humans, and no accurate method is currently available for assessment. Further studies to elucidate the mechanism on the effects of SGLT2 inhibitors on diabetic, but also non-diabetic, nephropathy are clearly needed.

Conclusion

In summary, two prerequisites are necessary to make a compound effective to sustainably activate the TGF system and sustainably alter renal hemodynamics. First, macula densa delivery should increase sustainably without any significant compensation in reabsorption in the segments upstream of the macula densa. Second, no compensation should occur in the TGF response. SGLT2 inhibitors seem to be the example of compounds that can activate the TGF system sustainably, which is one of the explanations for positive effects of SGLT2 inhibitors in advanced diabetic nephropathy as they decrease glomerular hyperfiltration by sustainably activating the TGF system. Besides, SGLT2 inhibitors can enhance network dynamics among NVUs and decrease ROS which can delay the progression of diabetic nephropathy. Finally, in diabetic patients, combination use of SGLT2 inhibitors and ARBs/ACEi could contribute to enhancement of renal hemodynamics. However, many questions remain regarding the exact mechanism of action of SGLT2 inhibitors.

Figure 1. Mechanisms contributing to the renal blood flow autoregulation. Transmission of an increase in arterial pressure to the afferent arteriole leads to the activation of MR and TGF to stabilize RBF and GFR. Activation of MR by a rise in afferent arteriole wall tension, due to increase in RBF results in afferent arteriole vasoconstriction to decrease RBF (B & C). Any residual rise in PGC and SNGFR after activation of MR, results in increase solute concentration of fluid reaching macula densa and secretion of adenosine and ATP, which leads to further constriction of the afferent arteriole and stabilization of PGC and SNGFR (B & C).

Figure 2. Compounds and conditions which sustainably activates the TGF mechanism. Compounds that decrease solute reabsorption in the proximal tubule/loop of Henle can sustainably increase macula densa delivery unless there is a compensation in the reabsorption in segments proximal to macula densa (Left). Sustained increase in macula densa delivery would lead to sustained activation of the TGF system unless there is a compensation in the TGF response (Right). Sustained activation of the TGF mechanism would result in sustained alteration of single nephron hemodynamics and presumable enhancement of synchronization among NVUs (Middle).

Figure 3. Nephrons' state, macula densa solute delivery and the TGF response in early and advanced diabetic nephropathy. A) Shows intact, hypertrophied nephrons in early diabetic nephropathy, which would result in increased solute reabsorption proximal to macula densa and deactivation of the TGF system and hyperfiltration. B_1) Shows intact hypertrophied nephrons in advanced diabetic nephropathy and how macula densa salute delivery and the TGF response might be changed based the extent of sclerosis in nearby nephrons. B_2) Shows partially sclerosed, hypertrophied nephrons in advanced diabetic nephropathy, which would result in decreased GFR and macula densa salute delivery and deactivation of the TGF system. B_3) Shows totally sclerosed nephrons and how they might affect nearby intact nephrons [99].

Renal Blood Flow Autoregulation

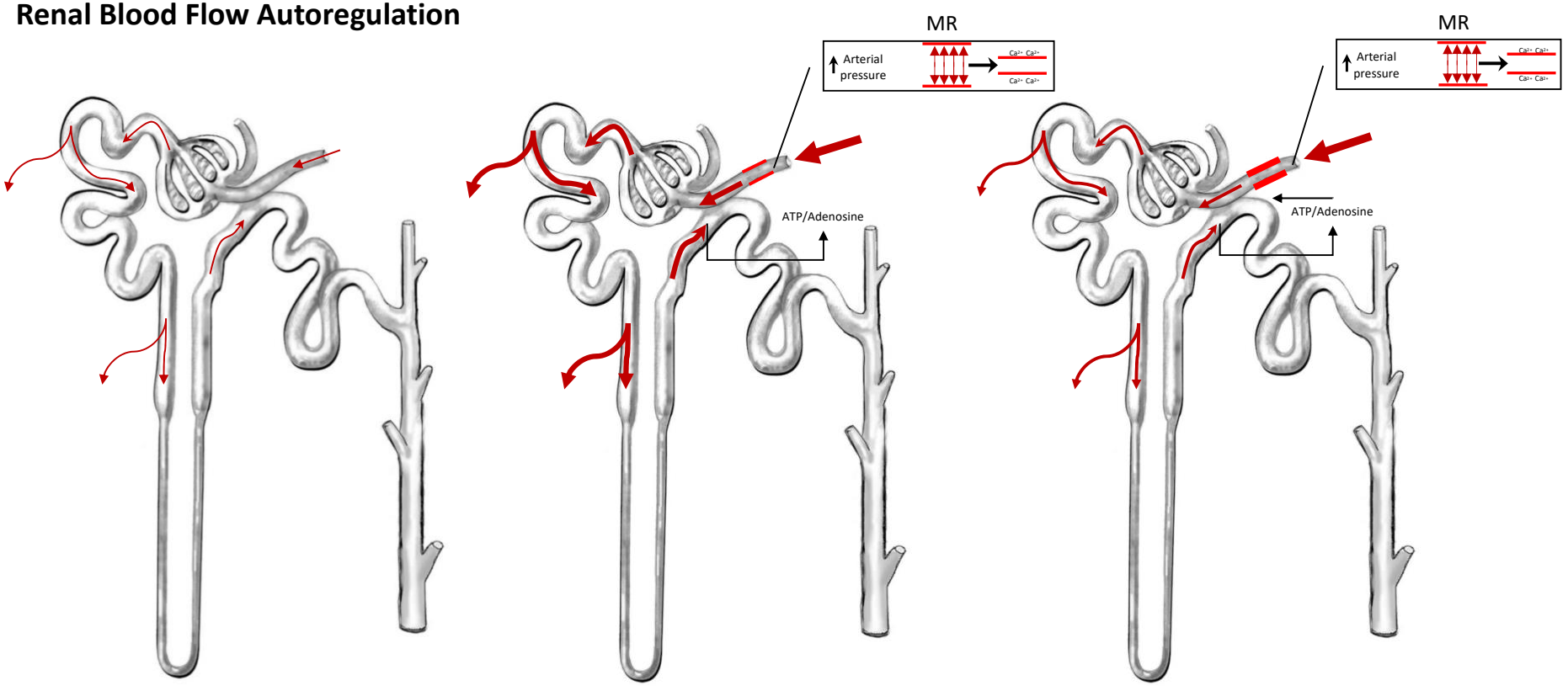

A B C

National Institute of Diabetes and Digestive and kidney diseases, National institutes of Health

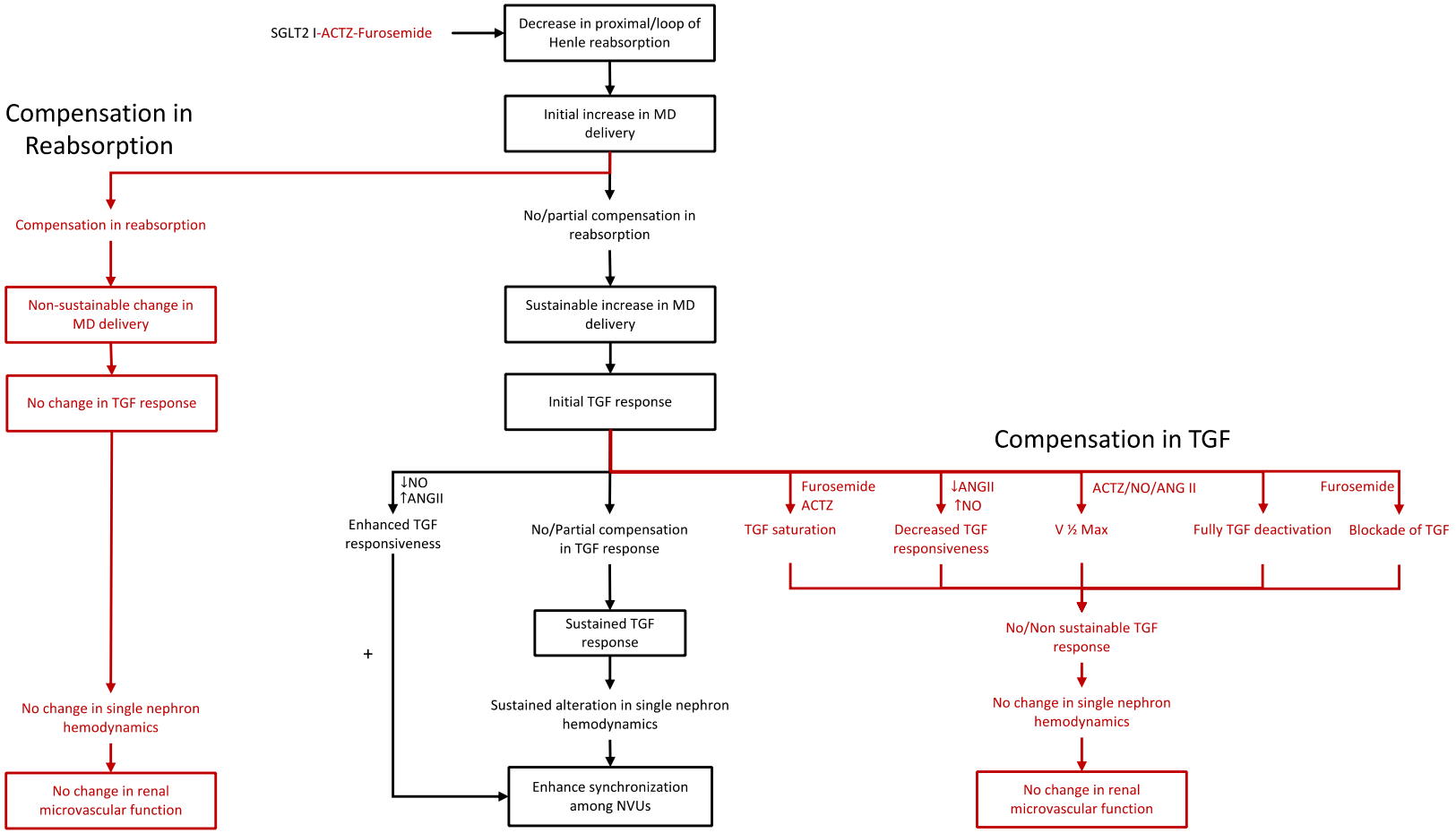
SGLT2 I-ACTZ-Furosemide
Decrease in proximal/loop of Henle reabsorption
Initial increase in MD delivery
Compensation in Reabsorption
Compensation in reabsorption
No/partial compensation in reabsorption
Non-sustainable change in MD delivery
Sustainable increase in MD delivery
No change in TGF response
Initial TGF response
Compensation in TGF
↓NO
↑ANGII
Enhanced TGF responsiveness
No/Partial compensation in TGF response
Furosemide
ACTZ
TGF saturation
↓ANGII
↑NO
Decreased TGF responsiveness
ACTZ/NO/ANG II
V ½ Max
Furosemide
Fully TGF deactivation
Blockade of TGF
Sustained TGF response
No/Non sustainable TGF response
+
Sustained alteration in single nephron hemodynamics
No change in single nephron hemodynamics
No change in single nephron hemodynamics
Enhance synchronization among NVUs
No change in renal microvascular function
No change in renal microvascular function

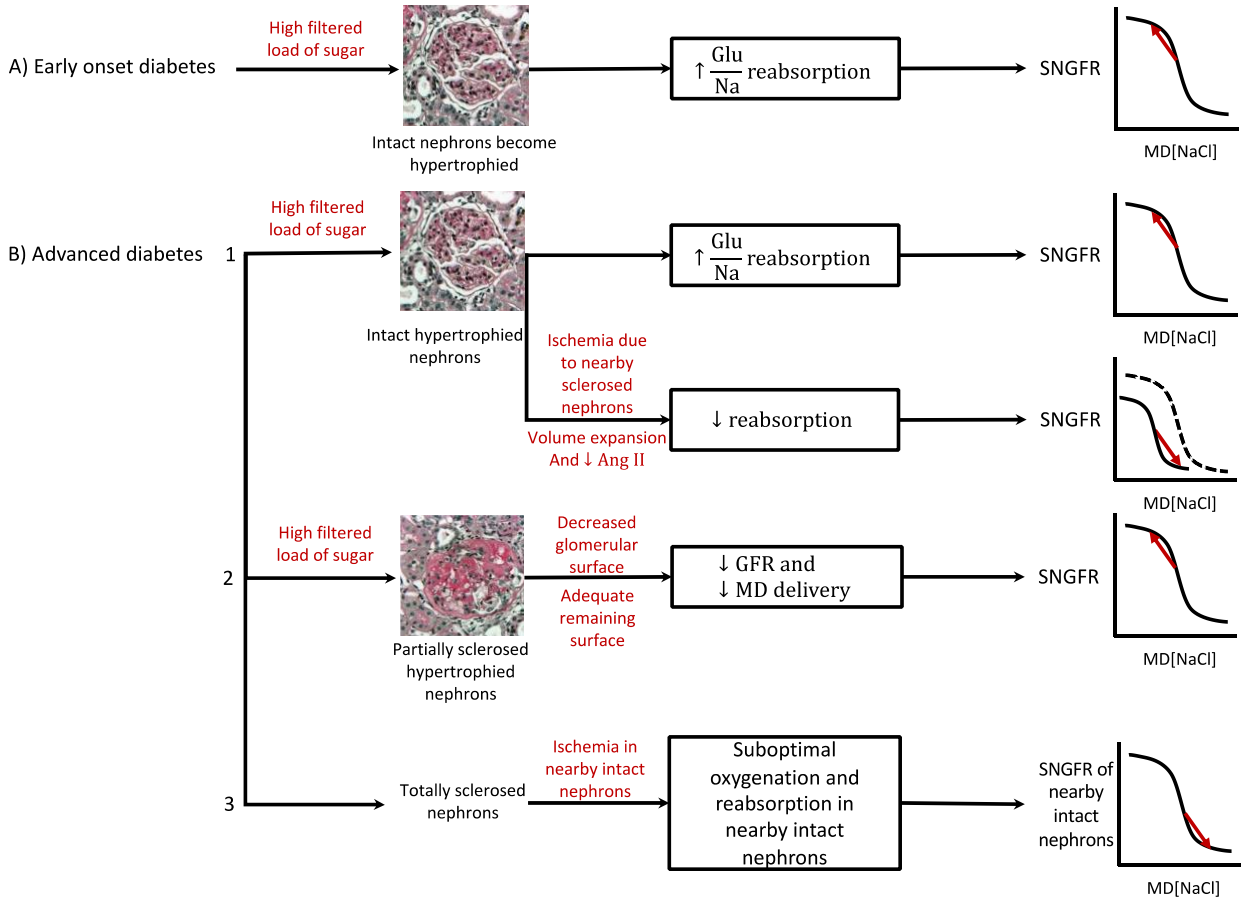
A) Early onset diabetes
High filtered load of sugar
Intact nephrons become hypertrophied
↑ Glu/Na reabsorption
SNGFR
MD[NaCl]
B) Advanced diabetes
1
High filtered load of sugar
Intact hypertrophied nephrons
↑ Glu/Na reabsorption
SNGFR
MD[NaCl]
Ischemia due to nearby sclerosed nephrons
Volume expansion And ↓ Ang II
↓ reabsorption
SNGFR
MD[NaCl]
2
High filtered load of sugar
Partially sclerosed hypertrophied nephrons
Decreased glomerular surface
Adequate remaining surface
↓ GFR and ↓ MD delivery
SNGFR
MD[NaCl]
3
Totally sclerosed nephrons
Ischemia in nearby intact nephrons
Suboptimal oxygenation and reabsorption in nearby intact nephrons
SNGFR of nearby intact nephrons
MD[NaCl]

Chapter 3: Methodology

Materials

All experiments were approved by the Animal Care Committee of the University of Alberta and were conducted according to the Canadian Council on Animal Care's guidelines. Male Lewis rats (350-450 g) (Charles River, St. Constant, QC, Canada) were housed in pairs with a 12:12 h light-dark cycle. Environment temperature and humidity were also controlled. Furthermore, all rats received regular rat chow and water ad libitum (Canadian Laboratory Diets, Leduc, AB, Canada).

Experimental procedure

Anesthesia was induced 20 min after subcutaneous administration of Buprenorphine (0.02 mg/kg) in a chamber using isoflurane (up to 4%) in 45% O2. Once the animal reached surgical plane, which was verified by checking the toe-pinch reflex, it was relocated to a thermo-feedback surgical table to keep temperature at 37°C (Vestavia Scientific, Birmingham, AL, USA). A cone was used to preserve anesthesia through the nose and the isoflurane dosage was slowly decreased to 2 % for the duration of the surgery and to 1.5% after the surgery (the lowest possible dose).

Hair from abdomen, left and right groin was shaved, and the surgical fields were cleaned by using 10% povidone iodine and 70% ethanol alternatively. After double checking surgical plane with the toe-pinch reflex, the surgery was started by cannulating the left femoral vein (Silastic tubing, 0.51 mm ID, 0.94 mm OD) for intravenous infusion of 5% bovine serum albumin (BSA) (A7906; Sigma, Oakville, ON) with 250 μg/min FITC inulin (Sigma) and 50 mM LiCl (Sigma) in 0.9% NaCl at 1.5 mL/h. The left femoral artery was also cannulated (PE-50; BD) for direct recording of mean arterial pressure and heart rate. Moreover, the right femoral vein was cannulated (Silastic tubing, 0.51 mm ID, 0.94 mm OD) for intravenous infusion of normal saline to replace plasma volume loss following furosemide/acetazolamide administration.

After midline laparotomy, the left kidney was uncovered, released from surrounding abdominal fat, and placed in a plastic kidney cup covered with silicone stopcock grease (Dow Corning, Midland, MI). The kidney was planted in silicone stopcock grease to minimize motion, and the kidney cup was connected to the surgical table. Additionally, the left renal artery was released from surrounding fat, and a transit time ultrasound flow probe (Transonic, Ithaca, NY) was placed around it to measure RBF. Acoustic coupling gel (SurgiLube, Transonic Systems, Ithaca, NY, USA) was used to secure the probe in place. In addition, the left ureter and bladder were cannulated for urine collection (PE-10; BD) (PE-90; BD). The kidney's surface was regularly humidified with normal saline except during imaging periods.

Experimental design

Equilibrium period (40-60 min)

Isoflurane was decreased to 1.5% in 45% O2 (the lowest possible dosage) and the intravenous infusion solution was switched to a mixture of 1% BSA with 250 μg/min FITC inulin and 50 mM LiCl in 0.9% NaCl at 1.5 mL/h during equilibration, and the animal was monitored for 40-60 min.

Baseline Period (60 min)

Following equilibration, and after cleaning the kidney surface with normal saline, the Moor FLPI LSI (Moore Instruments, Axminister, UK) was placed ~16-18 cm above the kidney surface. Then, a 4 mm hair was placed on the kidney surface to determine pixel size and to focus the LSI camera. Roughly one-third of the left kidney dorsal surface was imaged for 25 min for each spatial and temporal record and made two sets of each recording per experiment. During spatial record the

device was set to analyze a small group of pixels (5x5) within a single frame, acquiring 113 x 152-pixel images at 25 Hz. Additionally, during temporal record, the device was set to analyze single pixels over 25 frames, acquiring 760 x 568-pixel images at 1 Hz. Furthermore, left and right kidney urine was collected in pre-weighed tubes from the beginning of the baseline period for 30 minuets period until the end of the experiment. Blood was collected in the middle of the baseline and experimental period, which was used to collect plasma.

Furosemide/acetazolamide administration and equilibrium period (30 min)

A bolus of furosemide or acetazolamide were administered via the femoral vein. Following the bolus administration, the infusion solution was switched to 1% BSA with furosemide or acetazolamide in 250 µg/min FITC inulin, and 50 mM LiCl in 0.9% NaCl (1.5 ml/hr). The infusion rate from the second pump was determined over a 30 min period of equilibration following administration of the bolus by determining the volume of urine produced and was set accordingly.

This was based on the results from our lab done by Tayyaba Zehra; the urine flow after administrating 5 mg/kg furosemide is 60 μl/min, which leads to fluid loss of 3.6 ml/h. Moreover, plasma volume is 2.75% of the rat's weight (~400 g), which is almost 11 ml. Consequently, furosemide administration (5 mg/kg) leads to loss of one-third of plasma volume an hour, which should be replaced through administration of ringer lactate or normal saline [100]. Also, based on the results from Scott Thomson and his team [91], the urine flow after administrating 5 mg/kg benzolamide was ~ 35 μl/min, which leads to fluid loss of 1.8 ml/h. Consequently, acetazolamide administration leads to loss of 20% of plasma volume an hour, which should be replaced through administration of ringer lactate or normal saline [100].

Experimental period (60 min)

After equilibrium period (30 min), recording with LSI started again with two 25 min records in spatial and temporal averaging modes obtained. Left and right kidney urine was collected in pre-weighted tubes from the beginning of the experimental period for 30 minuets period until the end of the experiment. Blood was collected in the middle of the experimental period, which was used to collect plasma.

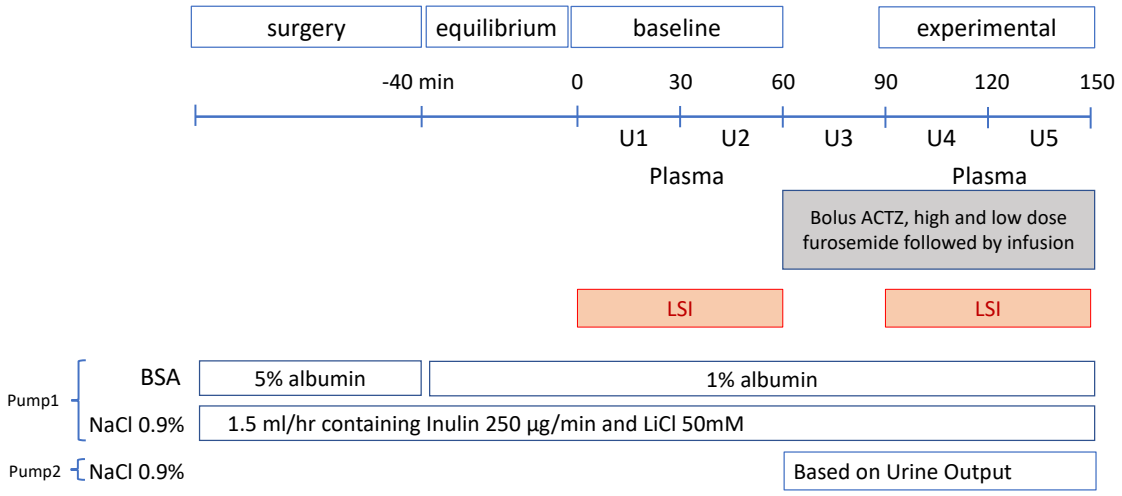

Figure 3.1. Experimental setup and infusion solutions. Rats were given 40 minuets to become stable after the surgery (equilibrium period). During baseline period, recording with LSI as well as collecting urine and plasma started. Then, diuretics were infused, followed by 30 equilibrium period. Finally, all the measurements during baseline period, including LSI recording, were repeated during experimental period.

Euthanasia

1.0 ml of pentobarbital sodium (Euthanyl; 240mg/ml) was injected intravenously to euthanize the rat, followed by cutting the heart mechanically.

Aim 1: Effects of administrating different dosage of furosemide on renal hemodynamics and synchronization among nearby nephrons

Intact rats (n=8) were prepared surgically, according to the previously approved protocol, to be given high dosage of furosemide (10, 20, 30 mg/kg). The number of rats given 10 mg/kg furosemide was four (n=4), while it was two for each of 20 (n=2) and 30 (n=2) mg/kg furosemide. All eight rats were included in the analysis.

Also, another group (n=3) of rats were prepared similarly to serve as the control group.

Aim 2: Effects of administrating high dose of acetazolamide on renal hemodynamics and synchronization among nearby nephrons

Intact rats (n=7) were prepared surgically, according to the previously approved protocol, to be infused high dosage of acetazolamide (10 mg/kg) intravenously. Another group of intact rats (n=4) were prepared similarly to serve as the vehicle group as acetazolamide was only soluble in DMSO.

One out of seven rats from the acetazolamide group was excluded from the analysis because of low blood pressure by the end of the surgery and the remaining rats were used for full analysis.

Acetazolamide preparation:

Acetazolamide (100 mg) (1005004; Sigma, Oakville, ON) was dissolved in 1 ml DMSO (Sigma) to prepare a master liquid (acetazolamide concentration was 100 mg/ml). For bolus infusion, the needed amount of master liquid was calculated based on rat's weight (10 mg/kg). Then, 10 ul tween 80 (Sigma) was added, followed by adding N/S to decrease DMSO concentration to 5%. For Infusion solution (total volume 3 ml), 0.2 ml BSA 15%, 0.72 ml LiCl (50 mM), 1 ml FITC

(3%) and 10 ul of tween 80 were added to the needed amount of master liquid (based on rat's weight). Finally, N/S was added to reach 3 ml volume.

Aim 3: Effects of administrating low dose of furosemide on renal hemodynamics and synchronization among nearby nephrons

Intact rats (n=6) were prepared surgically, according to the previously approved protocol, to be infused low dosage of furosemide (1 mg/kg) intravenously.

All 6 animals were included in the analysis.

Analytical procedures

Blood pressure, heart rate and renal blood flow

Blood pressure, heart rate and renal blood flow data were measured and saved on a PC using PowerLab Data Acquisition System (8/30; ADInstruments, Dunedin, NZ) and LabChart 6 Software.

Measurement of GFR

Rat plasma and urine (in pre-weighted tubes to measure urine volume) were collected. Inulin-FITC injection solution was diluted with HEPES to get the following standard dilution:

Inulin-FITC solution/total volume	Inulin-FITC injection solution
1:10	30ul undiluted solution
1:20	135ul (1:10) diluted solution
1:100	15ul (1:10) diluted solution
1: 200	15ul (1:20) diluted solution
1:1000	15ul (1:100) diluted solution
1:2000	15ul (1:200) diluted solution
1:10000	15ul (1:1000) diluted solution

Table 3.1. Preparation of Inulin-FITC standards. Inulin-FITC injection solution was diluted with HEPES to get the above standard dilutions.

Rat plasma or urine were diluted with HEPES:

- 25 ul plasma+100 ul HEPES
- 10 ul Urine + 190 ul HEPES

Measurement:

The samples were loaded onto a 96 well plate, 50ul/well. Fluorescence was determined using a Fluoroscan Ascent (Thermo Lab system), with 485nm excitation and read at 538nm emission. Standard readings were used to make standard curve which can be used to measure urine and plasma inulin concentrations (mg/ml).

GFR were calculated based on the clearance formula: GFR=CInulin=V*UInulin/PInulin

Strength of synchronization TGF

LSI is a non-invasive technique that measures superficial blood flow in tissues, and it can also be used to assess the strength of synchronization among nearby nephrons. LSI produces speckles which are interference patterns made by reflection of laser lights from the kidney surface. Movement of red blood cells through the superficial vasculature reduces speckles contrast and makes interference patterns. This is interpreted by LSI imager as alteration in local surface movement [4, 101, 102]. The real-time images produced by LSI can be used to assess the strength of synchronization among the nearby nephrons by calculating phase coherence, the number of edges with high phase coherence and decay of synchronization with distance.

1. *Phase coherence*

Phase coherence (PC) was calculated to assess the strength of the phase synchronization of TGF. To calculate PC, initially, each spatial record was filtered with a Gaussian spatial filter (8-pixel width) and down-sampled by a factor of 4 to get a 21*31-pixel image for each frame with average pixel of 135*135 um. Then, the TGF (0.015-0.06 Hz) frequency ranges were isolated via a bandpass forward-backward Butterworth filter [103]. Then, the Hilbert transform of each pixel timeseries was used to calculate the instantaneous phase. Then, we compared all possible pairs of imaged pixels to measure PC, where PCjk is the phase coherence between two pixels j and k. Also, N is the number of points in the original data, and ϕj and ϕk are the instantaneous phases of pixels j and k, respectively [103]. It is the mean of the exponential difference between the instantaneous phases of two pixels over time. PC is a number between 0 and 1, where PC = 0 means no relationship exists between two nodes (no synchronization), and PC = 1 indicates 100% phase locking between two nodes [103, 104].

$$PC_{jk} = \left| \frac{1}{N} \sum_{m=1}^{N} e^{i(\phi_j - \phi_k)} \right|$$

The calculations were done in a way that Pixel pairs with low PC (<0.5) were excluded from the analysis.

Increased mean PC means stronger synchronization, while lower PC shows weaker synchronization. While both spatial and temporal records can be used to calculate TGF PC, we used spatial records as they are more accurate in assessing TGF PC compared to temporal records.

2. *Number of edges:*

We also assessed long-distance synchronization between kidney regions by calculating the number of edges. To calculate this, graph analysis was used to restore the renal surface [105, 106]. In this graph, each pixel was recognized as a node. Pairs of nodes are connected if significant PC is existed between them, and this connection is recognized as an edge. An increase in the number of edges with high PC demonstrates stronger synchronization between regions of kidney. We only included edges with PC > 0.6 based on previous experiments that could detect edges with PC ≤ 0.6 in the absence of renal blood flow autoregulation [8, 68]. Also, as neighboring nodes have higher PC, which may affect the overall analysis, we excluded length of 1 and √2. Moreover, while both spatial and temporal records can be used to calculate the number of edges, we used spatial records as they are more common.

Decay of TGF synchronization with distance

We also used sum of exponentials model to find the relationship between PC and edge length, where A is the magnitude of the decay of PC over edge length, e is the base of natural logarithms, and K_1 and k2 K_2 are length constants [103].

$$PC = Ae^{\frac{length}{-k_1}} + e^{\frac{length}{-k_2}} - A$$

An increase in the magnitude of decay indicates weaker synchronization, while a decrease in magnitude of decay means stronger synchronization. Also, steeper decay in length constant associated with initial decay TGF_{PC} (K_1) indicates weaker synchronization within lobules, while steeper decay in length constant associated with secondary decay in TGF_{PC} (K_2) indicates weaker synchronization among neighboring lobules.

Statistical analysis

Hemodynamics variables and synchronizations parameters for all three aims were analyzed using Two Way repeated-measures ANOVA to account for the effect of time. Matlab (r2019a, The Mathworks, Natick, MA) was used to analyzed LSI data and statistical analysis performed in Excel 2016.

Chapter 4: Results

Aim 1: Effects of administering different dosage of furosemide on renal hemodynamics and synchronization among nearby nephrons

Blood pressure, renal blood flow and heart rate

Figure 4.1 shows mean arterial blood pressure (MAP), renal blood flow (RBF) and heart rate (HR) during baseline and after high dose (10, 20, 30 mg/kg) furosemide administration in intact male Lewis rats. MAP, RBF and HR were almost similar during baseline and after infusion of 10, 20, 30 mg/kg furosemide.

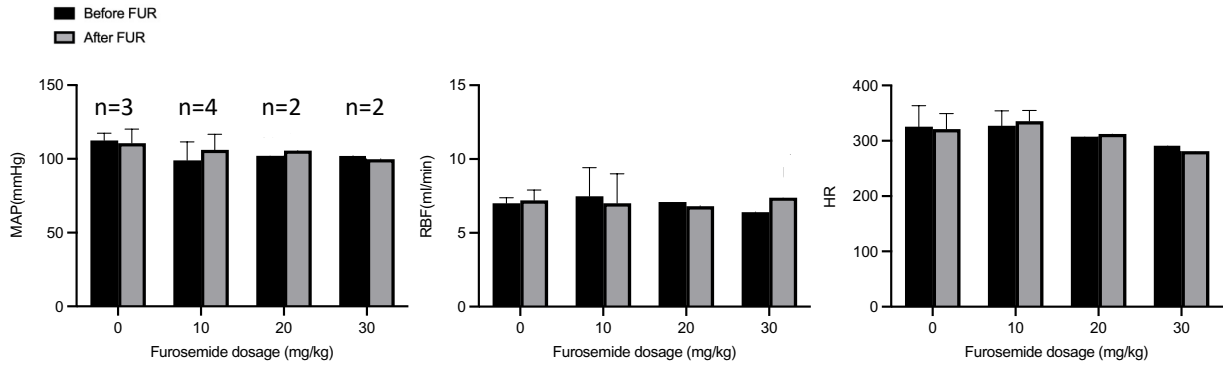

Figure 4.1. Mean arterial blood pressure (MAP), renal blood flow (RBF) and heart rate (HR) before and after administration of 0 (time-control), 10, 20, 30 mg/kg furosemide. MAP, RBF and HR were almost similar after administrating different dosage of furosemide.

Renal hemodynamics

Figure 4.2 shows renal vascular resistance (RVR) as well as right and left kidney GFR during baseline and after 10, 20, 30 mg/kg furosemide administration in intact male Lewis rats. These parameters were almost similar before and after administration of 10, 20, 30 mg/kg furosemide.

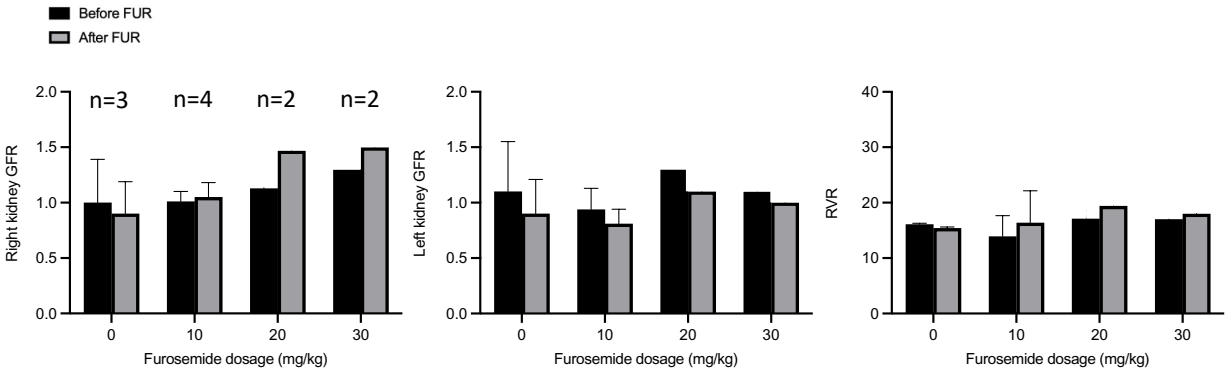

Figure 4.2. Right and left kidney GFR and renovascular resistance (RVR) before and after administration of 0 (time-control), 10, 20, 30 mg/kg furosemide. These parameters were almost similar before and after administration of different dosage of furosemide.

Figure 4.3 shows Left and right renal urine flow during baseline and after 10, 20, 30 mg/kg furosemide administration in intact male Lewis rats. Left and right renal urine production increased after administration of different dosage of furosemide.

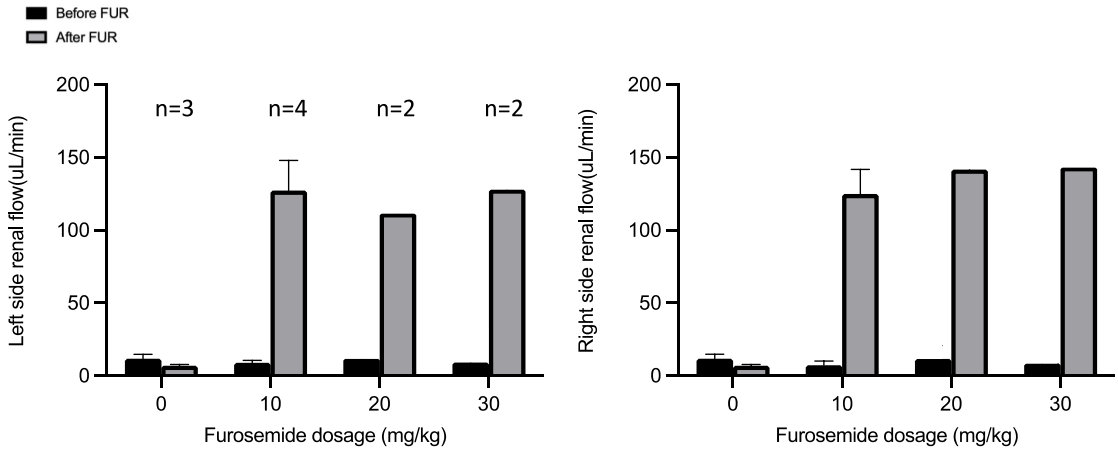

Figure 4.3. Left and right kidney urine flow before and after administration of 0 (time-control), 10, 20, 30 mg/kg furosemide. Urine flow increased after the intervention.

As the changes in MAP, RBF, HR, GFR, RVR and urine flow were almost the same before and after administration of different dosage of furosemide, we decided to pool the data to have a better understanding of the changes in these parameters before and after administration of high dosage furosemide. Table 4.1 summarizes MAP, HR, RBF, left and right kidney GFR, RVR and urine flow during baseline and after administration of high dose furosemide. RVR, right kidney GFR and urine flow increased after administration of high dose furosemide. However, left kidney GFR decreased. Other parameters did not change significantly.

	Before furosemide	After furosemide
MAP	100.6 ± 9.9	104.5 ± 9.2
HR	313 ± 25	316 ± 32
RBF	7.1 ± 2.3	6.9 ± 2.5
GFR (L)	1.06 ± 0.22	0.92 ± 0.16*
GFR (R)	1.10 ± 0.22	1.27 ± 0.27*
RVR	15.5 ± 4.9	17.5 ± 6.8*
Urine flow (R)	9.8 ± 3.1	123.5 ± 15.8†
Urine flow (L)	8.6 ± 4.6	133.7 ± 15.8†

Table 4.1. Values presented as mean ± SEM; n=8 high dose furosemide. Shown are MAP, HR, RBF, GFR, RVR as well as left and right-side urine flow. MAP; mean arterial pressure, HR; heart rate, RBF; renal blood flow, GFR; glomerular filtration rate, RVR; renal vascular resistance.

*$P < 0.5$, †$P < 0.001$ (Paired t-test).

Strength of TGF synchronization

Figure 4.4 shows mean PC and the number of edges, which can be used to assess strength of TGF synchronization, before and after administering of 10, 20, 30 mg/kg furosemide. Changes in mean PC and the number of edges were inconsistent after administration of high dose furosemide.

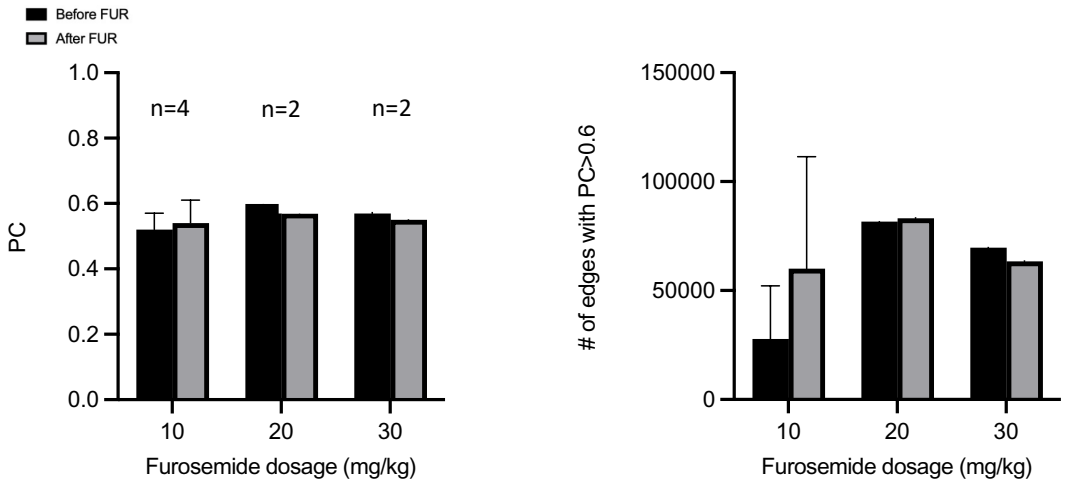

Figure 4.4. Mean phase coherence (PC) and the number of edges with high PC (PC > 0.6) before and after administration of 10, 20, 30 mg/kg furosemide. Changes in these two parameters were inconsistent after the intervention.

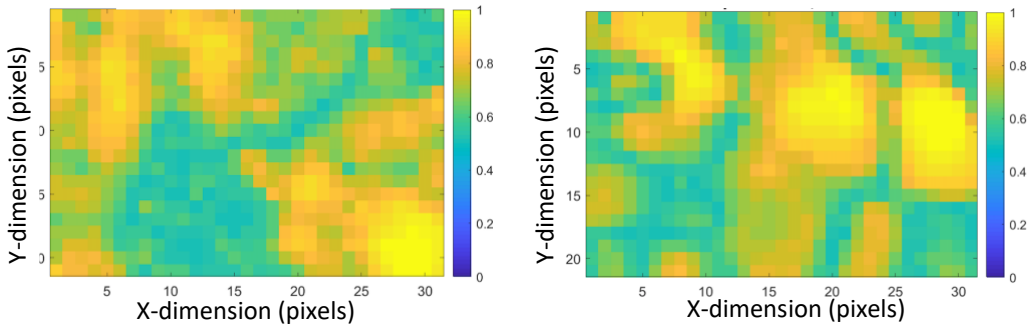

Figure 4.5. Graph indicates phase coherence of tubuloglomerular feedback synchronization at the kidney surface after administration of 20 mg/kg furosemide in a male Lewis rat. Results are from spatial speckle. Phase coherence (PC) ranges from 0 to 1 and shows strength of TGF synchronization. Moreover, LSI pixels are depicted as nodes and each node is connected to other nodes with an edge. Edges with PC > 0.6 are considered significant and are included in our analysis. More edges with PC > 0.6 indicate stronger synchronization at the kidney surface among nearby nephrovascular units. In this rat furosemide administration (20 mg/kg) did not change mean PC (0.494 to 0.495) or the number of edges with PC > 0.6 (18649 to 18276).

As the changes in mean PC and the number of edges were inconsistent after administration of different dosage of furosemide, we decided to pool the data to have a better understanding of the effects of high dose furosemide on mean PC and the number of edges. Table 4.2 summarizes variables that assess strength of TGF synchronization before and after administration of high dose furosemide. Mean PC and the number of edges with PC > 0.6 were used to assess the strength of TGF synchronization. High dose furosemide did not change mean PC and the number of edges significantly.

	Before furosemide	After furosemide
TGF (spatial speckle)		
Mean PC	0.55 ± 0.5	0.55 ± 0.5
# Of edges with PC > 0.6	51757 ± 35749	66679 ± 37291

Table 4.2. Values presented as mean ± SEM; n=8, high dose (10, 20, 30 mg/kg) furosemide. Shown are mean phase coherence (PC) and the number of edges with PC > 0.6. There were no

significant changes in these two parameters after administration of high dose furosemide (Paired t-test).

Decay of TGF synchronization with distance

Figure 4.6 shows the magnitude of decay of PC (A) associated with TGF as well as the initial (K_1) and secondary (K_2) decay of PC associated with TGF during baseline and after 10, 20, 30 mg/kg furosemide administration in intact male Lewis rats. Changes in A, K_1 and K_2 were inconsistent after injecting 10, 20, 30 mg/kg furosemide.

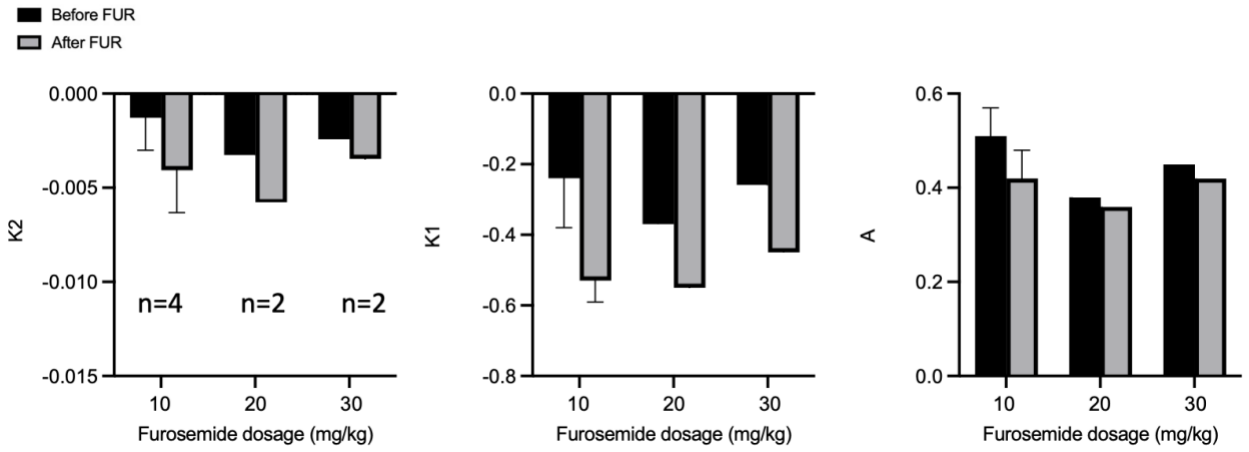

Figure 4.6. Magnitude of decay of PC (A) associated with TGF as well as initial (K_1) and secondary (K_2) decay of PC associated with TGF before and after administration 10, 20, 30 mg/kg furosemide. Changes in these parameters were inconsistent after infusion of high dose furosemide.

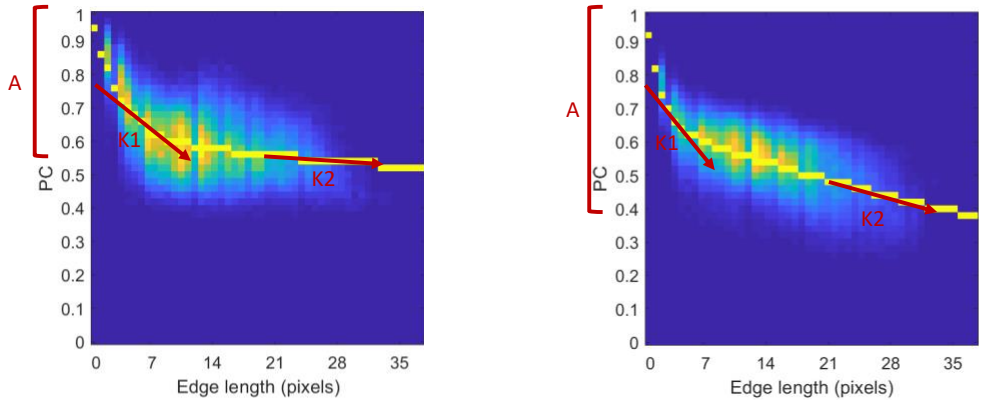

Figure 4.7. This figure shows the heatmap of the decay of TGF phase coherence with edge length after administration of high dose furosemide. These results are from spatial speckle. Yellow line shows the best-fit curve for the decay of TGF phase coherence. The magnitude of the decay (A) represents strength of synchronization: the higher the magnitude, the weaker the synchronization. Initial decay in TGF phase coherence (K_1) is associated with strength of synchronization within lobules: synchronization would be weaker within lobules if the initial decay is steeper. Furthermore, the secondary decay in TGF phase coherence (K_2) is associated with synchronization among neighboring lobules, synchronization would be weaker among neighboring lobules with steeper secondary decay. In this rat the magnitude of decay of TGF phase coherence, the initial decay of TGF phase coherence and the secondary decay of TGF phase coherence increased after administration of 20 mg/kg furosemide.

As the changes in A, K_1 and K_2 were inconsistent after administration of different dosage of furosemide, we decided to pool the data. Table 4.3 summarizes the magnitude of decay of PC associated with TGF as well as initial and secondary decay of PC associated with TGF (TGF_{PC}) synchronization before and after administration of high dose furosemide. High dose furosemide did not change the magnitude of decay of TGF_{PC} and secondary decay of TGF_{PC} significantly.

Additionally, initial decay of TGF_{PC} decreased significantly after the intervention, indicating weaker synchronization within lobules.

	Before furosemide	After furosemide
spatial speckle		
A	0.46 ± 0.08	0.42 ± 0.06
K_1	-0.28 ± 0.11	-0.53 ± 0.06*
K_2	-2.07 E-03 ± 1.51 E-03	4.07 E-03 ± 2.25 E-03

Table 4.3. Values presented as mean ± SEM; n=8, high dose (10, 20, 30 mg/kg) furosemide. Shown are the magnitude of decay of TGF PC (A), the phase coherence (PC) as well as initial (K_1) and secondary (K_2) decay of PC associated with TGF. K_1 decreased significantly after administrating high dosage of furosemide.

Aim 2: Effects of administering acetazolamide on renal hemodynamics and synchronization among nearby nephrons

Blood pressure, renal blood flow and heart rate

Figure 4.8 shows MAP, RBF and HR during baseline and after administration of 10 mg/kg acetazolamide in intact male Lewis rats. MAP and RBF decreased slightly after acetazolamide administration, while HR did not change significantly after infusion of 10 mg/kg acetazolamide.

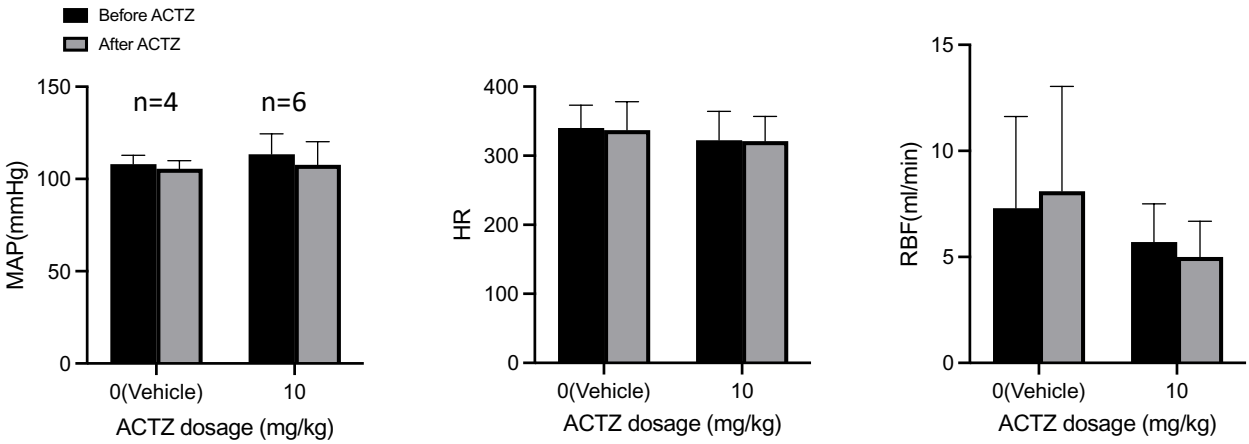

Figure 4.8. Mean arterial blood pressure (MAP), renal blood flow (RBF) and heart rate (HR) before and after administration of 10 mg/kg acetazolamide. MAP, RBF decreased marginally after administration of acetazolamide, while HR did not change significantly after administration of acetazolamide.

Renal hemodynamics

Figure 4.9 shows RVR as well as right and left kidney GFR during baseline and after administration of 10 mg/kg acetazolamide. Right and left kidney GFR decreased significantly after

infusion of acetazolamide (10 mg/kg) in intact male Lewis rats, while RVR did not change significantly after the intervention.

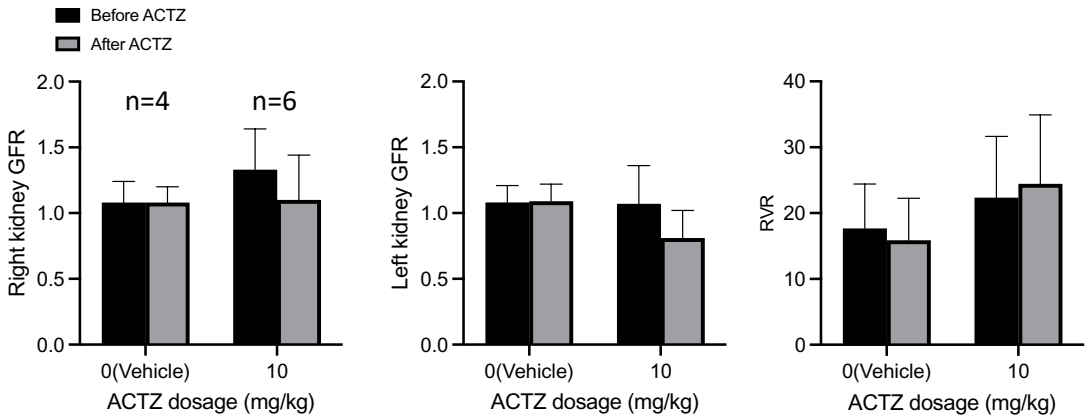

Figure 4.9. Right and left kidney GFR and renovascular resistance (RVR) before and after administration 10 mg/kg acetazolamide. Right and left kidney GFR decreased markedly after the intervention.

Figure 4.10 shows Left and right renal urine flow during baseline and after administration of 10 mg/kg acetazolamide. Left and right renal urine production increased significantly after administration of acetazolamide (10 mg/kg) in intact male Lewis rats.

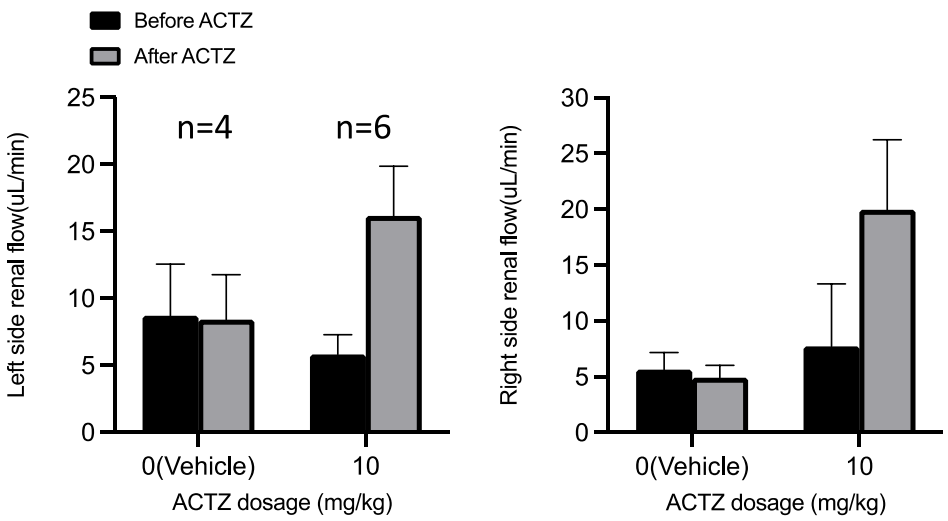

Figure 4.10. Left and right kidney urine flow before and after administration of 10 mg/kg acetazolamide. Acetazolamide increased left and right renal urine flow.

Table 4.4 summarizes changes in MAP, HR, RBF, GFR, RVR as well as right and left kidney urine flow during baseline and after administration of 10 mg/kg acetazolamide.

	Before acetazolamide	After acetazolamide
MAP	113.4 ± 11.0	107.7 ± 12.5*
HR	322 ± 41	321 ± 35
RBF	5.7 ± 1.8	5.0 ± 1.7*
GFR (L)	1.07 ± 0.29	0.81 ± 0.21*
GFR (R)	1.33 ± 0.31	1.10 ± 0.34*
RVR	25 ± 10	26.8 ± 11.7
Urine flow (L)	5.8 ± 1.5	16.2 ± 3.7†

Urine flow (R)	7.7 ± 5.6	19.9 ± 6.3*

Table 4.4. Values presented as mean ± SEM; n=6 10 mg/kg acetazolamide. Shown are MAP, HR, RBF, GFR, RVR as well as left and right-side urine flow. MAP, mean arterial pressure; HR, heart rate; RBF, renal blood flow; GFR, glomerular filtration rate; RVR, renal vascular resistance. *$P < 0.5$, †$P < 0.001$ (Paired t-test).

Strength and variability of synchronization

Figure 4.11 shows mean PC and the number of edges, which can be used to assess strength of TGF synchronization, during baseline and after administration of 10 mg/kg acetazolamide. The number of edges increased significantly after infusing acetazolamide. PC did not change significantly after the intervention.

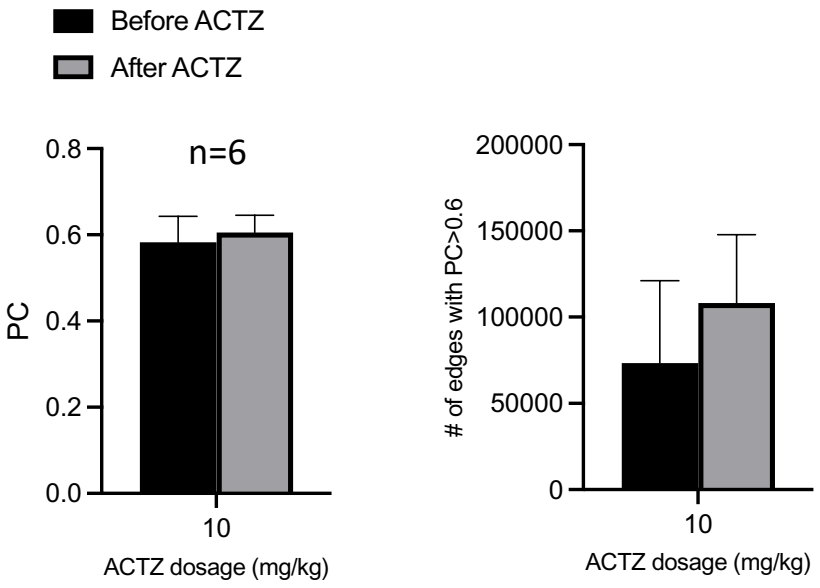

Figure 4.11. Mean phase coherence (PC) and the number of edges with high PC (PC > 0.6) before and after administration of 10 mg/kg acetazolamide. The number of edges with PC > 0.6 increased significantly after the intervention.

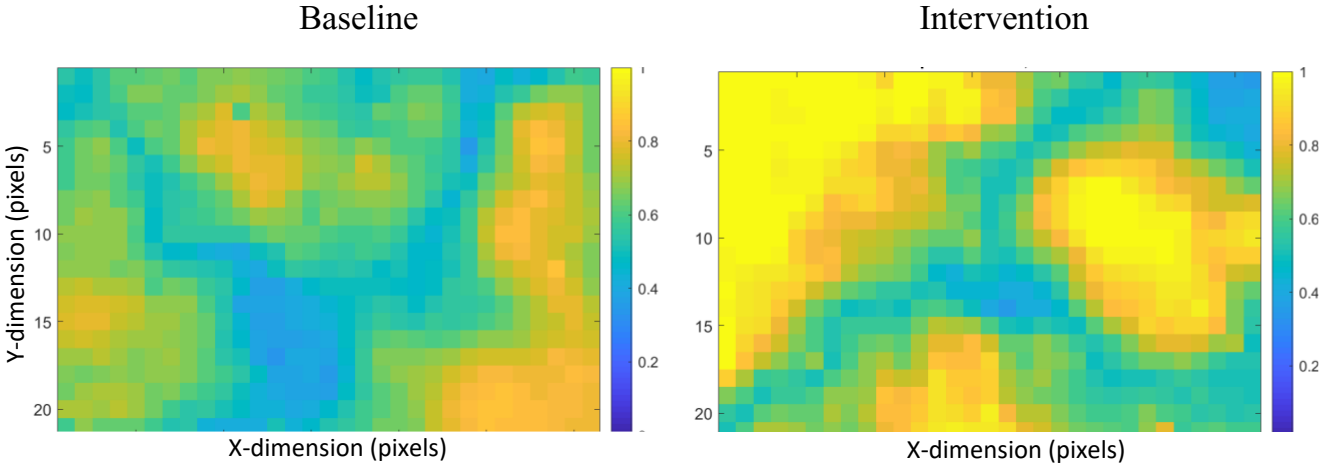

Figure 4.12. Graph indicates synchronization of TGF phase coherence after administration of 10 mg/kg acetazolamide in a male Lewis rat. Results are from spatial speckle. Phase coherence (PC) ranges from 0 to 1 and it shows strength of TGF synchronization. Moreover, LSI pixels are depicted as nodes and each node is connected other nodes with an edge. Edges with PC > 0.6 are considered significant and are included in our analysis. More edges with PC > 0.6 indicate stronger synchronization at the kidney surface among nearby nephrovascular units. In this rat acetazolamide administration (10 mg/kg) increased PC (0.53 to 0.63) and the number of edges with PC > 0.6 (39894 to 129546).

Table 4.5 summarizes variables that assess strength of TGF synchronization before and after administration of 10 mg/kg acetazolamide. Mean phase coherence (PC) and the number of edges

with high PC (PC > 0.6) were used to assess the strength of TGF synchronization. Acetazolamide increased the number of edges significantly.

	Before acetazolamide	After acetazolamide
TGF (spatial speckle)		
Mean PC	0.58 ± 0.06	0.61± 0.04
# Of edges with PC > 0.6	73221 ± 47292	108218 ± 39282*

Table 4.5. Values presented as mean ± SEM; n=6, 10 mg/kg acetazolamide. Shown are mean phase coherence (PC) and the number of edges with high PC. The number of edges with PC > 0.6 increased significantly after administration of acetazolamide.

Decay of TGF synchronization with distance

Figure 4.13 shows the magnitude of decay of PC (A) associated with TGF as well as initial (K_1) and secondary (K_1) decay of PC associated with TGF during baseline and after administration of 10 mg/kg acetazolamide. A decreased significantly after administering 10 mg/kg acetazolamide, while K_1 and K_2 did not change significantly after the intervention.

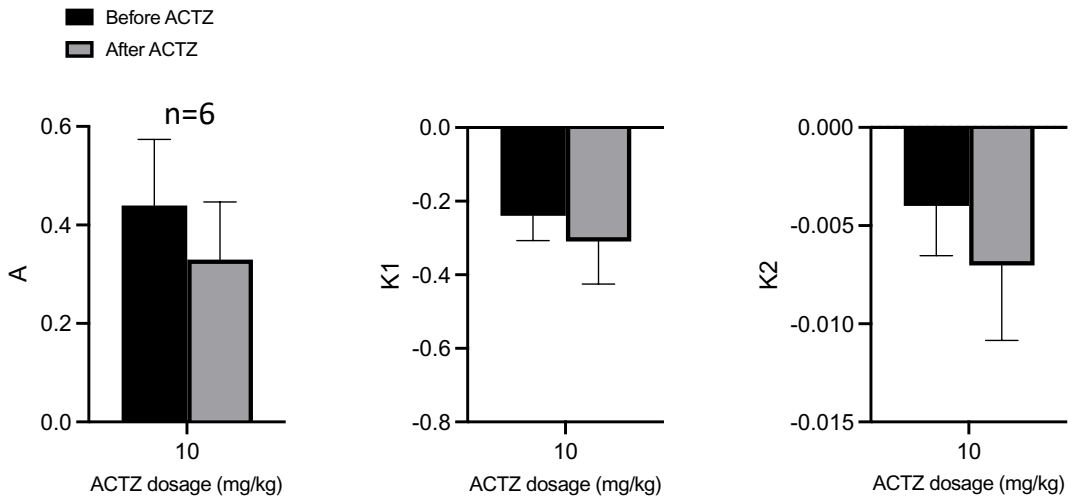

Figure 4.13. Magnitude of decay of PC (A) associated with TGF as well as initial (k1) and secondary (K_1) decay of PC associated with TGF before and after administration 10 mg/kg acetazolamide. A decreased significantly after the intervention. Changes in K_1 and K_2 were inconsistent after infusion of acetazolamide.

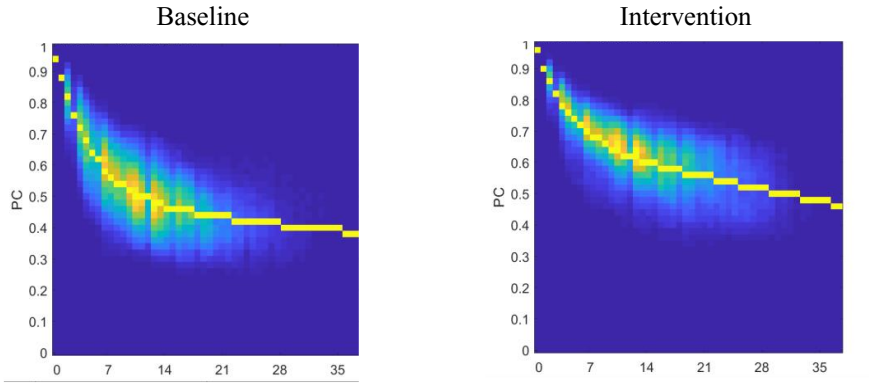

Figure 4.14. This figure shows the heatmap of the decay of TGF phase coherence with edge length after administration of acetazolamide. These results are from spatial speckle. Yellow line shows the best-fit curve for the decay of TGF phase coherence. The magnitude of the decay (A) represents strength of synchronization: the higher the magnitude, the weaker the synchronization. Initial decay in TGF phase coherence (K_1) is associated with strength of synchronization within lobules: synchronization is weaker within lobules if the initial decay is steeper. Furthermore, the secondary decay in TGF phase coherence (K_2) is associated with synchronization among neighboring lobules, synchronization is weaker among neighboring lobules with steeper secondary decay. In this rat the magnitude of decay of TGF phase coherence and the initial decay of TGF phase coherence decreased, whereas the secondary decay of TGF phase coherence remained almost the same after administration of 10 mg/kg acetazolamide.

Table 4.6 summarizes the magnitude of decay of PC associated with TGF as well as initial and secondary decay of PC associated with TGF during baseline and after administration of 10 mg/kg acetazolamide. Acetazolamide decreased the magnitude of decay of PC associated with TGF significantly. However, it did not change initial and secondary decay of PC associated with TGF (K_1 and K_2) significantly.

	Before acetazolamide	After acetazolamide
spatial speckle		
A	0.44 ± 0.13	0.33 ± 0.12*
K_1	-0.24 ± 0.07	-0.31 ± 0.16
K_2	-3.99E-03 ± 2.54 E-03	-7.94 E-03 ± 3.63 E-03

Table 4.6. Values presented as mean ± SEM; n=6, 10 mg/kg acetazolamide. Shown are the magnitude of decay of TGF PC (A) as well as the initial (K_1) and secondary (K_2) decay of PC associated with TGF. A decreased significantly after administrating acetazolamide, while K_1 and K_2 did not change significantly after acetazolamide administration.

Aim 3: Effects of administering low dose furosemide (1mg/kg) on renal hemodynamics and synchronization among nearby nephrons

Blood pressure, renal blood flow, heart rate and renal hemodynamics

Table 4.7 summarizes changes in MAP, HR, RBF, GFR (left), RVR as well as right and left kidney urine flow during baseline and after administering low dose of furosemide (1 mg/kg). RBF and GFR decreased after administration of low dose systemic furosemide. Furthermore, urine flow increased after the intervention. Other parameters did not change significantly after the intervention.

	Before furosemide	After furosemide
MAP	108.0 ± 6.1	105.9 ± 4.8
HR	362 ± 25	360 ± 23
RBF	5.9 ± 0.72	5.1 ± 0.34*
GFR (L)	1.19 ± 0.08	0.87 ± 0.12†
GFR (R)	1.23 ± 0.18	0.95 ± 0.10*
RVR	18.3 ± 1.6	20.8 ± 1.76*
Urine flow (L)	5.4 ± 0.96	19.1 ± 9.16*
Urine flow (R)	4.5 ± 0.52	13.6 ± 4.29*

Table 4.7. Values presented as mean ± SEM; n=6 low dose furosemide. Shown are MAP, HR, RBF, GFR, RVR as well as left and right-side urine flow. MAP, mean arterial pressure; HR, heart rate; RBF, renal blood flow; GFR, glomerular filtration rate; RVR, renal vascular resistance.

*$P < 0.5$, †$P < 0.001$ (Paired t-test).

Strength and variability of synchronization

Figure 4.15 shows mean PC and the number of edges, which can be used to assess strength of TGF synchronization, during baseline and after administration of 1 mg/kg furosemide. PC and the number of edges with PC > 0.6 increased after administering 1 mg/kg furosemide.

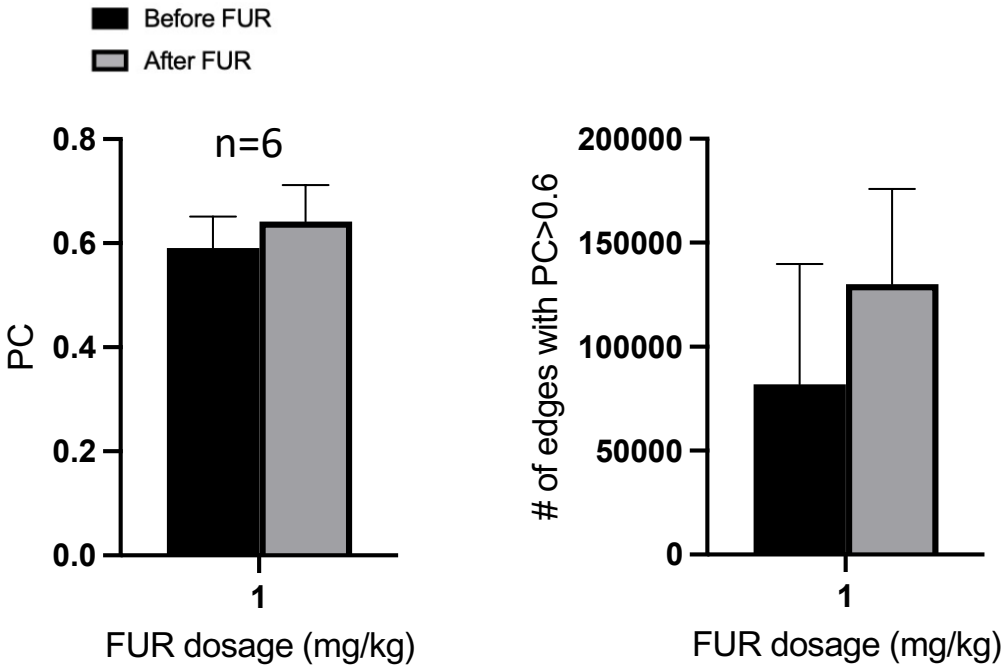

Figure 4.15. Phase coherence (PC) and the number of edges with high PC (PC > 0.6) before and after administration low dose furosemide. These two parameters increased after infusion of low dose furosemide.

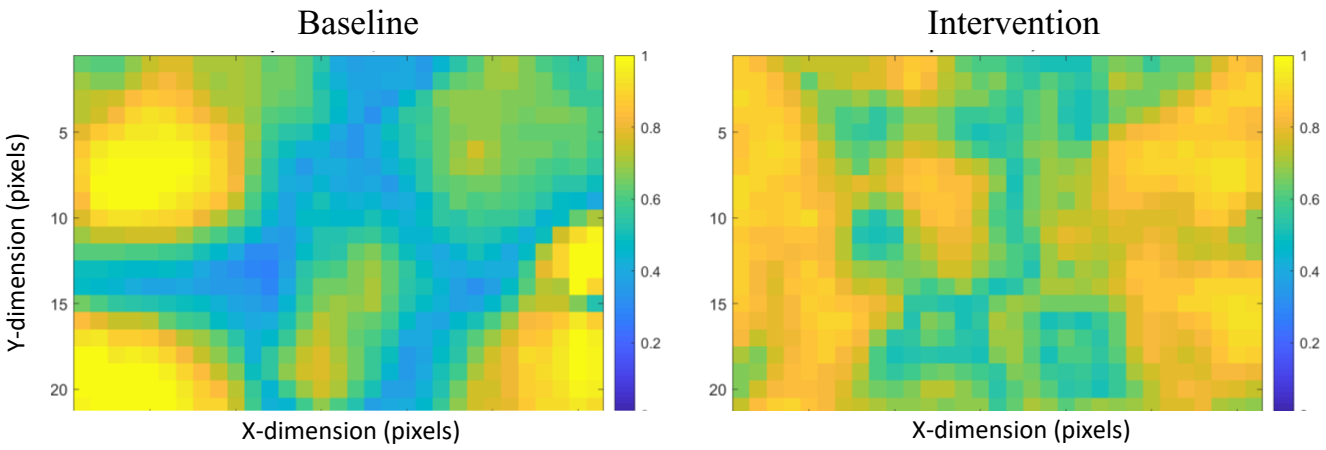

Figure 4.16. Graph indicates synchronization of TGF phase coherence after administration of 1 mg/kg furosemide in a rat. Results are from spatial speckle. Phase coherence (PC) ranges from 0 to 1 and it shows strength of TGF synchronization. Moreover, LSI pixels are depicted as nodes and each node is connected other nodes with an edge. Edges with PC > 0.6 are considered significant and are included in our analysis. More edges with PC > 0.6 indicate stronger synchronization at the kidney surface among nearby nephrovascular units. In this rat furosemide administration (1 mg/kg) increased PC (0.55 to 0.58) and the number of edges with PC > 0.6 (62521 to 92540).

Table 4.8 summarizes variables that assess strength of TGF synchronization before and during administration of low dose furosemide. Mean phase coherence (PC) and the number of edges with high PC (PC > 0.6) were used to assess the strength of TGF synchronization. Low dose furosemide increased mean PC and the number of edges with high PC significantly.

	Before furosemide	After furosemide
TGF (spatial speckle)		
Mean PC	0.59 ± 0.06	0.64± 0.07*
# Of edges with PC > 0.6	81867 ± 57903	130007 ± 45935*

Table 4.8. Values presented as mean ± SEM; n=6, 1 mg/kg furosemide. Shown are mean phase coherence (PC) and the number of edges with high PC. There were significant increase in both of these two parameters after administration of furosemide. $^{*}P < 0.5$ (Paired t-test).

Decay of TGF synchronization with distance

Figure 4.17 shows the magnitude of decay of PC (A) associated with TGF as well as initial (K_1) and secondary (K_1) decay of PC associated with TGF during baseline and after administration of 1 mg/kg furosemide. A decreased after administration of low dose furosemide, while K_1 and K_2 did not change significantly after administering 1 mg/kg furosemide.

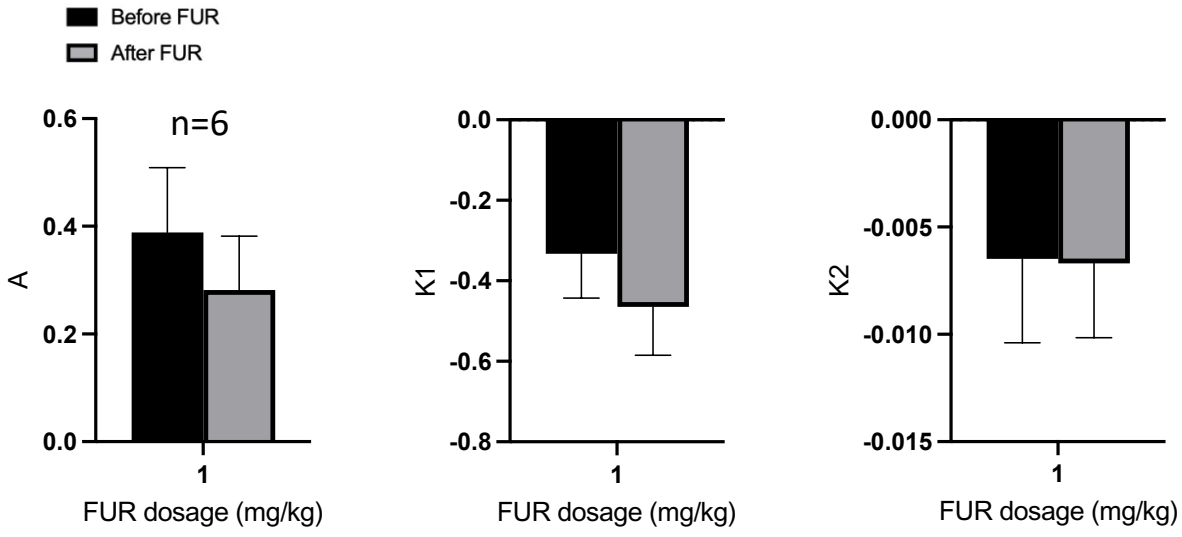

Figure 4.17. Magnitude of decay of PC (A) associated with TGF as well as initial (k1) and secondary (K_1) decay of PC associated with TGF before and after administration of 1 mg/kg furosemide. A decreased after infusion of low dose furosemide while changes in K_1 and K_2 were inconsistent.

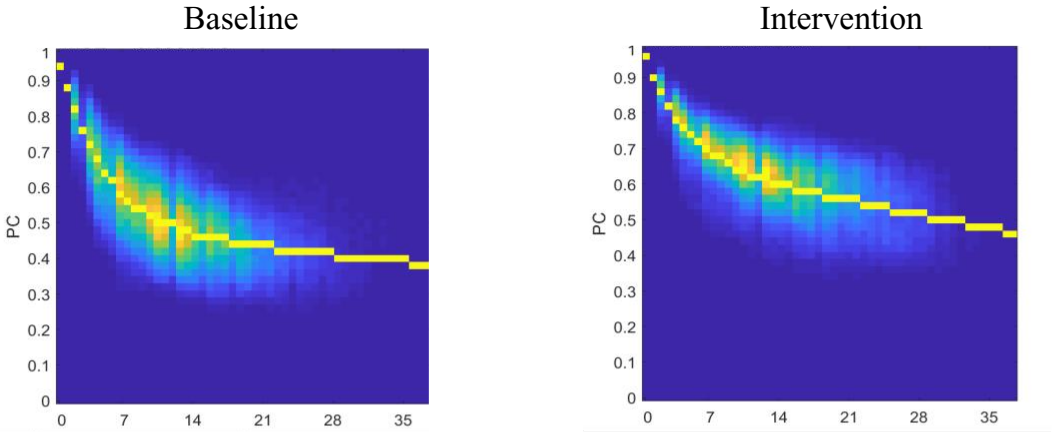

Figure 4.18. This figure shows the heatmap of the decay of TGF phase coherence with edge length after administration of low dose furosemide. These results are from spatial speckle. Yellow line shows the best-fit curve for the decay of TGF phase coherence. The magnitude of the decay (A) represents strength of synchronization: the higher the magnitude, the weaker the synchronization. Initial decay in TGF phase coherence (K_1) is associated with strength of synchronization within lobules: synchronization is weaker within lobules if the initial decay is steeper. Furthermore, the secondary decay in TGF phase coherence (K_2) is associated with synchronization among neighboring lobules, synchronization is weaker among neighboring lobules with steeper secondary decay. In this rat the magnitude of decay of TGF phase coherence and the initial decay of TGF phase coherence decreased, whereas the secondary decay of TGF phase coherence remained almost the same after administration of 1 mg/kg furosemide.

Table 4.9 summarizes the magnitude of decay of PC associated with TGF as well as initial and secondary decay of PC associated with TGF during baseline and after administration of 1 mg/kg furosemide. Low dose furosemide decreased the magnitude of decay of PC associated with TGF significantly. However, it did not change initial and secondary decay of PC associated with TGF significantly.

	Before furosemide	After furosemide
spatial speckle		
A	0.39 ± 0.12	0.28 ± 0.10†
K_1	-0.33 ± 0.11	-0.47 ± 0.12
K_2	-6.48E-03 ± 3.96E-03	-6.69E-03 ± 3.47E-03

Table 4.9. Values presented as mean ± SEM; n=6, low dose (10 mg/kg) furosemide. Shown are the magnitude of decay of TGF PC (A), the phase coherence (PC) as well as initial (K_1) and secondary (K_2) decay of PC associated with TGF. A decreased significantly after administering furosemide, while K_1 and K_2 did not change significantly after low dose furosemide administration †$P < 0.001$ (Paired t-test).

Chapter 5: Discussion, Conclusion and Perspectives

5.1 General discussion

The main purpose of this research work was to get a better understanding of synchronization (coupling) among NVUs. We hypothesized that synchronization among nearby NVUs, each nephron and its afferent and efferent arterioles, would increase by activating TGF, while inhibiting TGF would decrease synchronization among NVUs. Consequently, in our first aim we tested the effects of administering systemic high dose furosemide, which can inhibit the TGF sensing step, on synchronization among NVUs. We hypothesized that synchronization would decrease among nearby NVUs after administrating high dose furosemide. Furthermore, in our second and third aims, we tested the effects of administrating low dose systemic furosemide and acetazolamide, which can increase macula densa solute delivery and activate the TGF, on synchronization among nearby NVUs. We hypothesized that these two compounds can enhance synchronization among nearby NVUs.

In the first aim, the changes in RBF, GFR, PC, the number of edges and the magnitude of decay of TGF_{PC} were inconsistent, showing the complexity of high dose furosemide. This is likely a result of variable inhibition of the NKCC2 (the sensing step of the TGF) by high dose furosemide as well as the role of other factors such as ANG II and/or NO on the TGF responsiveness and synchronization among NVUs. In the second and third aim, we observed parallel decrease in RBF and GFR, indicating activation of TGF. We also observed increased PC, the number of edges and decreased magnitude of decay of TGF_{PC} after administration of low dose furosemide and acetazolamide indicating enhancement of coupling among nearby NVUs.

These results provide a new insight about the autoregulation of renal blood flow among synchronized NVUs via the TGF mechanism. This was achieved using LSI, which captures cortical perfusion and provides information about synchronization among nearby NVUs [8, 103]. This was the first project assessing the effects of acetazolamide as well as significantly high and low dose furosemide on coupling among NVUs.

Renal hemodynamics

Aim 1 & 3: In several studies assessing the effects of administering furosemide on RBF and GFR in healthy subjects, the results were variable and inconsistent. In most of the studies, GFR increased or remained stable [107-111], while in some studies GFR decreased [112, 113]. RBF also increased, decreased, or remained constant in different studies [110, 114-116]. This demonstrates the complexity of furosemide's hemodynamic effects. In our study, RBF and whole kidney GFR in male Lewis rats remained almost constant after administering high dose furosemide, which was also reported by Tucker and Blantz [117]. Low dose furosemide, however, led to a parallel decrease in RBF and GFR, indicating activation of TGF and afferent arteriole vasoconstriction by low dose furosemide, which was also reported by Braam [9].

Altogether, the inconsistency of furosemide's hemodynamic effects is likely a result of variable inhibition of the NKCC2 (the sensing step of the TGF) by high dose furosemide as well as the role of other factors such as ANG II and/or NO on the TGF responsiveness. Moreover, it was shown by Loutezenhiser group that furosemide impairs MR [118]. This also renders RBF autoregulatory behavior ineffective and can explain inconsistent and variable changes in RBF and GFR after administering high dose of furosemide.

Aim 2: Carbonic anhydrase inhibitors can increase macula densa solute delivery, activate the TGF and decrease RBF and GFR. In our study intravenous administration of carbonic anhydrase inhibitor (acetazolamide), decreased both RBF and GFR significantly, indicating activation of TGF. These findings were consistent with other studies in animals and humans [87, 88, 90, 119]

Strength and variability of synchronization

Aim 1: It was expected that high dose furosemide inhibits the sensing step of the TGF (NKCC2 transporters at macula densa) and consequently decrease synchronization among nearby NVUs. However, high dose furosemide did not change RBF, GFR, PC and the number of edges, indicating no TGF activation and no changes in synchronization among nearby NVUs. Similar results were also reported by our group (Tayyaba Zehra) after administrating 5 mg/kg furosemide. This can be likely due to the three following explanations: 1) Partial inhibition of the NKCC2 transporters at macula densa as significantly high tubular concentration of furosemide is needed to block NKCC2 transporters at macula densa [9]. We infused a substantial high dosage of furosemide to saturate the NKCC2 transporters at loop of Henle and inhibit NKCC2 at macula densa. While, in some of our experiments TGF was inhibited and synchronization decreased, we did not see consistent results. 2) Furosemide leads to an increase in circulating renin and ANG II levels, which would result in an increase in reabsorption upstream of macula densa. ANG II also increases TGF responsiveness [9]. We tried to replenish volume loss using normal saline to reduce the effects of activation of RAS on proximal reabsorption and TGF responsiveness. However, volume loss was variable in different rats and assessing the exact amount of volume loss was challenging, which could have resulted in over/under infusion of normal saline. This could lead to activation of RAS/NOS and affect proximal reabsorption and the TGF. 3) Furosemide was shown to impair

MR, which can make the RBF autoregulation ineffective [118], rendering RBF, GFR unchanged and affect synchronization among nearby NVUs.

Aim 2: It was expected that acetazolamide increases macula densa solute delivery, activates the TGF and enhance synchronization among nearby NVUs, which was also seen in our experiments. Acetazolamide decreased both RBF and GFR, indicating activation of TGF. It also increased PC and the number of edges consistently, indicating enhancement of synchronization among nearby NVUs.

Aim 3: We expected that low dose systemic furosemide increases macula densa solute delivery and activate the TGF and enhance synchronization among nearby NVUs, which was also observed in our experiments. Low dose systemic furosemide decreased both RBF and GFR, indicating TGF activation. Moreover, low dose systemic furosemide increased PC and the number of edges, indicating enhancement of synchronization among nearby NVUs.

Decay of TGF synchronization with distance

The magnitude of decay of TGF_{PC} as well as the initial and secondary decay of TGF_{PC} give us more information about the strength of synchronization among NVUs. The magnitude of decay of TGF_{PC} is associated with strength of synchronization, the lower the magnitude, the stronger the synchronization. Moreover, the initial decay of TGF_{PC} is associated with synchronization within nearby lobules; synchronization would be lower within lobules if the initial decay is steeper. Furthermore, the secondary decay of TGF_{PC} is associated with synchronization with neighboring lobules; synchronization would be lower among neighboring lobules with steeper secondary decay

Aim 1: High dose furosemide caused a steeper decay in the initial decay associated with TGF_{PC}, which can reflect weaker synchronization within nearby lobules. Additionally, it was expected that high dose furosemide increases the magnitude of decay of TGF_{PC}. However, the magnitude of decay of TGF_{PC} decreased after administration of high dose furosemide, indicating enhancement of synchronization. Overall, combining these findings with changes of PC, the number of edges and renal hemodynamics indicates inconsistent effects of systemic high dose furosemide on TGF and synchronization among NVUs.

Aim 2 & 3: Acetazolamide and low dose systemic furosemide decreased the magnitude of decay of TGF_{PC} significantly, indicating enhancement of TGF synchronization. Combination of these results with changes in PC and the number of edges can be interpreted as stronger TGF synchronization among nearby NVUs after administrating acetazolamide and low dose systemic furosemide.

There are some limitations in the study. The variability in the number of edges and PC was an ongoing problem. The pixel size that our FLPI LSI device captures is 8 x 8 um. Each pixel in the image shows an area of the kidney surface and LSI measures the motion in a pixel. Movements of the kidney surface due to pulse or/and respiration would also be captured by the LSI, which could affect the number of edges and PC. Moreover, there are some biological variations between different rats, which can also affect the TGF and synchronization among NVUs. Furthermore, in the Aim 1 assessing the effects of high dose systemic furosemide on renal hemodynamics and synchronization among nearby NVUs, urine flow was more than 7 ml/h, which is more than 50%

of plasma volume. We tried to replenish the volume loss by infusing normal saline via a second pump and adjust the infusion rate every 10 minuets. However, a small decrease and increase in plasma volume would result in activation of RAS and/or NOS respectively, which might affect solute reabsorption proximal to macula densa and TGF responsiveness. Moreover, in aim 2, mean PC increased slightly in all experiments consistently. However, we did not see statistically significant increase in this parameter, possibly due to low sample number.

5.2 Conclusion

These experiments showed that furosemide is a complex compound. Furosemide:

- Increases distal solute delivery.
- Changes TGF responsiveness.
- Causes vasodilation.
- Increases renin and ANG II levels.

It is likely that other factors such as ANG II and NO affect TGF responsiveness and synchronization among NVUS during administration of systemic high dose furosemide. Moreover, inhibition of MR by high dose furosemide could affect RBF autoregulation and synchronization among NVUs.

We demonstrated for the first time that low dose furosemide and acetazolamide can enhance synchronization among NVUs:

- Administration of both compounds resulted in parallel decrease in RBF and GFR, indicating activation of TGF.
- Increased PC and the number of edges as well as decreased the magnitude of decay of TGF_{PC}, indicating increased synchronization among nearby NVUs at the kidney surface.

5.3 Perspectives

This study states that synchronization among NVUs occurs across the kidneys. We illustrated that low dose systemic furosemide and acetazolamide can enhance synchronization among NVUs at the kidney surface. Moreover, weakening of synchronization among NVUs was observed in some of our experiments administrating high dose systemic furosemide. All together, these experiments demonstrated the presence of synchronization among NVUs and the possibility to enhance it in the kidneys. This can be used to preserve renal function and prevent progression of diabetic and non-diabetic nephropathy in patients.

The next steps can be assessing the effects of low dose furosemide, dapagliflozin and the combination of these medications on synchronization among NVUs in intact and CKD models in rats. This would help to see whether combination of these two compounds can have a superior effects on synchronization among NVUs.

References

1. Arora, P., et al., *Prevalence estimates of chronic kidney disease in Canada: results of a nationally representative survey.* CMAJ, 2013. **185**(9): p. E417-23.
2. Just, A. and W.J. Arendshorst, *Dynamics and contribution of mechanisms mediating renal blood flow autoregulation.* Am J Physiol Regul Integr Comp Physiol, 2003. **285**(3): p. R619-31.
3. Cupples, W.A. and B. Braam, *Assessment of renal autoregulation.* Am J Physiol Renal Physiol, 2007. **292**(4): p. F1105-23.
4. Zehra, T., W.A. Cupples, and B. Braam, *Tubuloglomerular Feedback Synchronization in Nephrovascular Networks.* J Am Soc Nephrol, 2021. **32**(6): p. 1293-1304.
5. Yip, K.P., N.H. Holstein-Rathlou, and D.J. Marsh, *Dynamics of TGF-initiated nephron-nephron interactions in normotensive rats and SHR.* Am J Physiol, 1992. **262**(6 Pt 2): p. F980-8.
6. Holstein-Rathlou, N.H., *Synchronization of proximal intratubular pressure oscillations: evidence for interaction between nephrons.* Pflugers Arch, 1987. **408**(5): p. 438-43.
7. Leyssac, P.P. and L. Baumbach, *An oscillating intratubular pressure response to alterations in Henle loop flow in the rat kidney.* Acta Physiol Scand, 1983. **117**(3): p. 415-9.
8. Mitrou, N., B. Braam, and W.A. Cupples, *A gap junction inhibitor, carbenoxolone, induces spatiotemporal dispersion of renal cortical perfusion and impairs autoregulation.* Am J Physiol Heart Circ Physiol, 2016. **311**(3): p. H582-91.
9. Huang, X., et al., *Everything we always wanted to know about furosemide but were afraid to ask.* Am J Physiol Renal Physiol, 2016. **310**(10): p. F958-71.

10. Wheeler, D.C., et al., *Effects of dapagliflozin on major adverse kidney and cardiovascular events in patients with diabetic and non-diabetic chronic kidney disease: a prespecified analysis from the DAPA-CKD trial.* Lancet Diabetes Endocrinol, 2021. **9**(1): p. 22-31.

11. Heerspink, H.J.L., et al., *Dapagliflozin in Patients with Chronic Kidney Disease.* N Engl J Med, 2020. **383**(15): p. 1436-1446.

12. Cherney, D.Z., et al., *Renal hemodynamic effect of sodium-glucose cotransporter 2 inhibition in patients with type 1 diabetes mellitus.* Circulation, 2014. **129**(5): p. 587-97.

13. Thomson, S.C., et al., *Acute and chronic effects of SGLT2 blockade on glomerular and tubular function in the early diabetic rat.* Am J Physiol Regul Integr Comp Physiol, 2012. **302**(1): p. R75-83.

14. Thomson, S.C. and V. Vallon, *Renal Effects of Sodium-Glucose Co-Transporter Inhibitors.* Am J Cardiol, 2019. **124 Suppl 1**: p. S28-S35.

15. Vallon, V. and S.C. Thomson, *Targeting renal glucose reabsorption to treat hyperglycaemia: the pleiotropic effects of SGLT2 inhibition.* Diabetologia, 2017. **60**(2): p. 215-225.

16. Perkovic, V., et al., *Canagliflozin and Renal Outcomes in Type 2 Diabetes and Nephropathy.* N Engl J Med, 2019. **380**(24): p. 2295-2306.

17. Yip, K.P., N.H. Holstein-Rathlou, and D.J. Marsh, *Mechanisms of temporal variation in single-nephron blood flow in rats.* Am J Physiol, 1993. **264**(3 Pt 2): p. F427-34.

18. Daniels, F.H. and W.J. Arendshorst, *Tubuloglomerular feedback kinetics in spontaneously hypertensive and Wistar-Kyoto rats.* Am J Physiol, 1990. **259**(3 Pt 2): p. F529-34.

19. Casellas, D. and L.C. Moore, *Autoregulation and tubuloglomerular feedback in juxtamedullary glomerular arterioles.* Am J Physiol, 1990. **258**(3 Pt 2): p. F660-9.

20. Steinhausen, M., et al., *Visualization of renal autoregulation in the split hydronephrotic kidney of rats.* Kidney Int, 1989. **35**(5): p. 1151-60.

21. Moore, L.C. and D. Casellas, *Tubuloglomerular feedback dependence of autoregulation in rat juxtamedullary afferent arterioles.* Kidney Int, 1990. **37**(6): p. 1402-8.

22. Takenaka, T., et al., *Autoregulation of afferent arteriolar blood flow in juxtamedullary nephrons.* Am J Physiol, 1994. **267**(5 Pt 2): p. F879-87.

23. Van Dokkum, R.P., et al., *Impaired autoregulation of renal blood flow in the fawn-hooded rat.* Am J Physiol, 1999. **276**(1): p. R189-96.

24. Ploth, D.W., et al., *Autoregulation and tubuloglomerular feedback in normotensive and hypertensive rats.* Kidney Int, 1977. **12**(4): p. 253-67.

25. Aukland, K. and A.H. Oien, *Renal autoregulation: models combining tubuloglomerular feedback and myogenic response.* Am J Physiol, 1987. **252**(4 Pt 2): p. F768-83.

26. Just, A. and W.J. Arendshorst, *A novel mechanism of renal blood flow autoregulation and the autoregulatory role of A1 adenosine receptors in mice.* Am J Physiol Renal Physiol, 2007. **293**(5): p. F1489-500.

27. Hashimoto, S., et al., *Reduced autoregulatory effectiveness in adenosine 1 receptor-deficient mice.* Am J Physiol Renal Physiol, 2006. **290**(4): p. F888-91.

28. Walker, M., 3rd, et al., *Dynamic interaction between myogenic and TGF mechanisms in afferent arteriolar blood flow autoregulation.* Am J Physiol Renal Physiol, 2000. **279**(5): p. F858-65.

29. Flemming, B., et al., *Time-dependent autoregulation of renal blood flow in conscious rats.* J Am Soc Nephrol, 2001. **12**(11): p. 2253-62.

30. Biemesderfer, D., et al., *Monoclonal antibodies for high-resolution localization of NHE3 in adult and neonatal rat kidney.* Am J Physiol, 1997. **273**(2 Pt 2): p. F289-99.

31. Biemesderfer, D., et al., *NHE3: a Na+/H+ exchanger isoform of renal brush border.* Am J Physiol, 1993. **265**(5 Pt 2): p. F736-42.

32. Preisig, P.A., et al., *Role of the Na+/H+ antiporter in rat proximal tubule bicarbonate absorption.* J Clin Invest, 1987. **80**(4): p. 970-8.

33. Preisig, P.A. and F.C. Rector, Jr., *Role of Na+-H+ antiport in rat proximal tubule NaCl absorption.* Am J Physiol, 1988. **255**(3 Pt 2): p. F461-5.

34. Vallon, V., et al., *Role of Na(+)/H(+) exchanger NHE3 in nephron function: micropuncture studies with S3226, an inhibitor of NHE3.* Am J Physiol Renal Physiol, 2000. **278**(3): p. F375-9.

35. Moe, O.W., *Acute regulation of proximal tubule apical membrane Na/H exchanger NHE-3: role of phosphorylation, protein trafficking, and regulatory factors.* J Am Soc Nephrol, 1999. **10**(11): p. 2412-25.

36. Baum, M., et al., *Glucocorticoids regulate NHE-3 transcription in OKP cells.* Am J Physiol, 1996. **270**(1 Pt 2): p. F164-9.

37. Klisic, J., et al., *Insulin activates Na(+)/H(+) exchanger 3: biphasic response and glucocorticoid dependence.* Am J Physiol Renal Physiol, 2002. **283**(3): p. F532-9.

38. Collazo, R., et al., *Acute regulation of Na+/H+ exchanger NHE3 by parathyroid hormone via NHE3 phosphorylation and dynamin-dependent endocytosis.* J Biol Chem, 2000. **275**(41): p. 31601-8.

39. Crajoinas, R.O., et al., *Angiotensin II counteracts the effects of cAMP/PKA on NHE3 activity and phosphorylation in proximal tubule cells.* Am J Physiol Cell Physiol, 2016. **311**(5): p. C768-C776.

40. Donowitz, M. and X. Li, *Regulatory binding partners and complexes of NHE3.* Physiol Rev, 2007. **87**(3): p. 825-72.

41. Bobulescu, I.A. and O.W. Moe, *Luminal Na(+)/H (+) exchange in the proximal tubule.* Pflugers Arch, 2009. **458**(1): p. 5-21.

42. Pessoa, T.D., et al., *Functional role of glucose metabolism, osmotic stress, and sodium-glucose cotransporter isoform-mediated transport on Na+/H+ exchanger isoform 3 activity in the renal proximal tubule.* J Am Soc Nephrol, 2014. **25**(9): p. 2028-39.

43. Onishi, A., et al., *A role for tubular Na(+)/H(+) exchanger NHE3 in the natriuretic effect of the SGLT2 inhibitor empagliflozin.* Am J Physiol Renal Physiol, 2020. **319**(4): p. F712-F728.

44. Vallon, V., et al., *SGLT2 mediates glucose reabsorption in the early proximal tubule.* J Am Soc Nephrol, 2011. **22**(1): p. 104-12.

45. Hummel, C.S., et al., *Glucose transport by human renal Na+/D-glucose cotransporters SGLT1 and SGLT2.* Am J Physiol Cell Physiol, 2011. **300**(1): p. C14-21.

46. Poulsen, S.B., R.A. Fenton, and T. Rieg, *Sodium-glucose cotransport.* Curr Opin Nephrol Hypertens, 2015. **24**(5): p. 463-9.

47. Vallon, V., *The proximal tubule in the pathophysiology of the diabetic kidney.* Am J Physiol Regul Integr Comp Physiol, 2011. **300**(5): p. R1009-22.

48. Freitas, H.S., et al., *Na(+) -glucose transporter-2 messenger ribonucleic acid expression in kidney of diabetic rats correlates with glycemic levels: involvement of hepatocyte nuclear factor-1alpha expression and activity.* Endocrinology, 2008. **149**(2): p. 717-24.

49. Ghezzi, C. and E.M. Wright, *Regulation of the human Na+-dependent glucose cotransporter hSGLT2.* Am J Physiol Cell Physiol, 2012. **303**(3): p. C348-54.

50. Ares, G.R., P.S. Caceres, and P.A. Ortiz, *Molecular regulation of NKCC2 in the thick ascending limb.* Am J Physiol Renal Physiol, 2011. **301**(6): p. F1143-59.

51. Mount, D.B., *Thick ascending limb of the loop of Henle.* Clin J Am Soc Nephrol, 2014. **9**(11): p. 1974-86.

52. Hennings, J.C., et al., *The ClC-K2 Chloride Channel Is Critical for Salt Handling in the Distal Nephron.* J Am Soc Nephrol, 2017. **28**(1): p. 209-217.

53. Zacchia, M., et al., *The importance of the thick ascending limb of Henle's loop in renal physiology and pathophysiology.* Int J Nephrol Renovasc Dis, 2018. **11**: p. 81-92.

54. Palmer, L.G. and J. Schnermann, *Integrated control of Na transport along the nephron.* Clin J Am Soc Nephrol, 2015. **10**(4): p. 676-87.

55. Nielsen, S., et al., *Aquaporin-1 water channels in short and long loop descending thin limbs and in descending vasa recta in rat kidney.* Am J Physiol, 1995. **268**(6 Pt 2): p. F1023-37.

56. Kim, W.Y., et al., *Descending thin limb of the intermediate loop expresses both aquaporin 1 and urea transporter A2 in the mouse kidney.* Histochem Cell Biol, 2016. **146**(1): p. 1-12.

57. Mutig, K., et al., *Vasopressin V2 receptor expression along rat, mouse, and human renal epithelia with focus on TAL.* Am J Physiol Renal Physiol, 2007. **293**(4): p. F1166-77.

58. Ramseyer, V.D., et al., *Angiotensin II-mediated hypertension impairs nitric oxide-induced NKCC2 inhibition in thick ascending limbs.* Am J Physiol Renal Physiol, 2016. **310**(8): p. F748-F754.

59. Silva, G.B. and J.L. Garvin, *Angiotensin II-dependent hypertension increases Na transport-related oxygen consumption by the thick ascending limb.* Hypertension, 2008. **52**(6): p. 1091-8.

60. Fernandez-Llama, P., et al., *Cyclooxygenase inhibitors increase Na-K-2Cl cotransporter abundance in thick ascending limb of Henle's loop.* Am J Physiol, 1999. **277**(2): p. F219-26.

61. Vallon, V., et al., *Glomerular hyperfiltration in experimental diabetes mellitus: potential role of tubular reabsorption.* J Am Soc Nephrol, 1999. **10**(12): p. 2569-76.

62. Vallon, V., et al., *Knockout of Na-glucose transporter SGLT2 attenuates hyperglycemia and glomerular hyperfiltration but not kidney growth or injury in diabetes mellitus.* Am J Physiol Renal Physiol, 2013. **304**(2): p. F156-67.

63. Thomson, S.C., V. Vallon, and R.C. Blantz, *Kidney function in early diabetes: the tubular hypothesis of glomerular filtration.* Am J Physiol Renal Physiol, 2004. **286**(1): p. F8-15.

64. Min, S.H., et al., *Association of angiotensin-II levels with albuminuria in subjects with normal glucose metabolism, prediabetes, and type 2 diabetes mellitus.* J Diabetes Complications, 2017. **31**(10): p. 1499-1505.

65. Satou, R., et al., *Blockade of sodium-glucose cotransporter 2 suppresses high glucose-induced angiotensinogen augmentation in renal proximal tubular cells.* Am J Physiol Renal Physiol, 2020. **318**(1): p. F67-F75.

66. Kamiyama, M., A. Zsombok, and H. Kobori, *Urinary angiotensinogen as a novel early biomarker of intrarenal renin-angiotensin system activation in experimental type 1 diabetes.* J Pharmacol Sci, 2012. **119**(4): p. 314-23.

67. Miyata, K., et al., *Sequential activation of the reactive oxygen species/angiotensinogen/renin-angiotensin system axis in renal injury of type 2 diabetic rats.* Clin Exp Pharmacol Physiol, 2008. **35**(8): p. 922-7.

68. Mitrou, N., et al., *Transient impairment of dynamic renal autoregulation in early diabetes mellitus in rats.* Am J Physiol Regul Integr Comp Physiol, 2015. **309**(8): p. R892-901.

69. Mogensen, C.E., *Early glomerular hyperfiltration in insulin-dependent diabetics and late nephropathy.* Scand J Clin Lab Invest, 1986. **46**(3): p. 201-6.

70. Braam, B., L.G. Navar, and K.D. Mitchell, *Modulation of tubuloglomerular feedback by angiotensin II type 1 receptors during the development of Goldblatt hypertension.* Hypertension, 1995. **25**(6): p. 1232-7.

71. Boer, W.H., et al., *Effects of reduced renal perfusion pressure and acute volume expansion on proximal tubule and whole kidney angiotensin II content in the rat.* Kidney Int, 1997. **51**(1): p. 44-9.

72. Braam, B., et al., *Relevance of the tubuloglomerular feedback mechanism in pathophysiology.* J Am Soc Nephrol, 1993. **4**(6): p. 1257-74.

73. Bhatt, D.L., et al., *Sotagliflozin in Patients with Diabetes and Chronic Kidney Disease.* N Engl J Med, 2021. **384**(2): p. 129-139.

74. Rieg, T., et al., *Increase in SGLT1-mediated transport explains renal glucose reabsorption during genetic and pharmacological SGLT2 inhibition in euglycemia.* Am J Physiol Renal Physiol, 2014. **306**(2): p. F188-93.

75. Zhang, J., et al., *Macula Densa SGLT1-NOS1-Tubuloglomerular Feedback Pathway, a New Mechanism for Glomerular Hyperfiltration during Hyperglycemia.* J Am Soc Nephrol, 2019. **30**(4): p. 578-593.

76. Wilcox, C.S., *Antihypertensive and Renal Mechanisms of SGLT2 (Sodium-Glucose Linked Transporter 2) Inhibitors.* Hypertension, 2020. **75**(4): p. 894-901.

77. Braam, B., *Renal endothelial and macula densa NOS: integrated response to changes in extracellular fluid volume.* Am J Physiol, 1999. **276**(6): p. R1551-61.

78. Braam, B. and H.A. Koomans, *Nitric oxide antagonizes the actions of angiotensin II to enhance tubuloglomerular feedback responsiveness.* Kidney Int, 1995. **48**(5): p. 1406-11.

79. Cupples, W.A., *Angiotensin II conditions the slow component of autoregulation of renal blood flow.* Am J Physiol, 1993. **264**(3 Pt 2): p. F515-22.

80. Turkstra, E., B. Braam, and H.A. Koomans, *Nitric oxide release as an essential mitigating step in tubuloglomerular feedback: observations during intrarenal nitric oxide clamp.* J Am Soc Nephrol, 1998. **9**(9): p. 1596-603.

81. Sorensen, C.M., et al., *Role of the renin-angiotensin system in regulation and autoregulation of renal blood flow.* Am J Physiol Regul Integr Comp Physiol, 2000. **279**(3): p. R1017-24.

82. Holm, L., et al., *Resetting of the pressure range for blood flow autoregulation in the rat kidney.* Acta Physiol Scand, 1990. **138**(3): p. 395-401.

83. Ploth, D.W., et al., *Tubuloglomerular feedback and single nephron function after converting enzyme inhibition in the rat.* J Clin Invest, 1979. **64**(5): p. 1325-35.

84. Turkstra, E., B. Braam, and H.A. Koomans, *Normal TGF responsiveness during chronic treatment with angiotensin-converting enzyme inhibition: role of AT1 receptors.* Hypertension, 2000. **36**(5): p. 818-23.

85. Krishnan, D., et al., *Carbonic anhydrase II binds to and increases the activity of the epithelial sodium-proton exchanger, NHE3.* Am J Physiol Renal Physiol, 2015. **309**(4): p. F383-92.

86. Hashimoto, S., et al., *Effect of carbonic anhydrase inhibition on GFR and renal hemodynamics in adenosine-1 receptor-deficient mice.* Pflugers Arch, 2004. **448**(6): p. 621-8.

87. Leyssac, P.P., et al., *On determinants of glomerular filtration rate after inhibition of proximal tubular reabsorption.* Am J Physiol, 1994. **266**(5 Pt 2): p. R1544-50.

88. Skott, P., et al., *The acute effect of acetazolamide on glomerular filtration rate and proximal tubular reabsorption of sodium and water in normal man.* Scand J Clin Lab Invest, 1989. **49**(6): p. 583-7.

89. Deng, A., J.S. Hammes, and S.C. Thomson, *Hemodynamics of early tubuloglomerular feedback resetting during reduced proximal reabsorption.* Kidney Int, 2002. **62**(6): p. 2136-43.

90. Thomson, S.C., et al., *Temporal adjustment of the juxtaglomerular apparatus during sustained inhibition of proximal reabsorption.* J Clin Invest, 1999. **104**(8): p. 1149-58.

91. Thomson, S.C., V. Vallon, and R.C. Blantz, *Reduced proximal reabsorption resets tubuloglomerular feedback in euvolemic rats.* Am J Physiol, 1997. **273**(4): p. R1414-20.

92. Ichihara, A. and L.G. Navar, *Neuronal NOS contributes to biphasic autoregulatory response during enhanced TGF activity.* Am J Physiol, 1999. **277**(1): p. F113-20.

93. Tsimihodimos, V., T.D. Filippatos, and M.S. Elisaf, *SGLT2 inhibitors and the kidney: Effects and mechanisms.* Diabetes Metab Syndr, 2018. **12**(6): p. 1117-1123.

94. Jhuo, S.J., et al., *Characteristics of Ventricular Electrophysiological Substrates in Metabolic Mice Treated with Empagliflozin.* Int J Mol Sci, 2021. **22**(11).

95. Vallon, V., et al., *SGLT2 inhibitor empagliflozin reduces renal growth and albuminuria in proportion to hyperglycemia and prevents glomerular hyperfiltration in diabetic Akita mice.* Am J Physiol Renal Physiol, 2014. **306**(2): p. F194-204.

96. Yaribeygi, H., et al., *Sodium-glucose cotransporter 2 inhibitors and inflammation in chronic kidney disease: Possible molecular pathways.* J Cell Physiol, 2018. **234**(1): p. 223-230.

97. Lo, C.S., et al., *Dual RAS blockade normalizes angiotensin-converting enzyme-2 expression and prevents hypertension and tubular apoptosis in Akita angiotensinogen-transgenic mice.* Am J Physiol Renal Physiol, 2012. **302**(7): p. F840-52.

98. Shi, Y., et al., *Angiotensin-(1-7) prevents systemic hypertension, attenuates oxidative stress and tubulointerstitial fibrosis, and normalizes renal angiotensin-converting enzyme 2 and Mas receptor expression in diabetic mice.* Clin Sci (Lond), 2015. **128**(10): p. 649-63.

99. Sima, C.A., et al., *Increased susceptibility to hypertensive renal disease in streptozotocin-treated diabetic rats is not modulated by salt intake.* Diabetologia, 2012. **55**(8): p. 2246-55.

100. Maddox, D.A., D.C. Price, and F.C. Rector, Jr., *Effects of surgery on plasma volume and salt and water excretion in rats.* Am J Physiol, 1977. **233**(6): p. F600-6.

101. Dunn, A.K., *Laser speckle contrast imaging of cerebral blood flow.* Ann Biomed Eng, 2012. **40**(2): p. 367-77.

102. Senarathna, J., et al., *Laser Speckle Contrast Imaging: theory, instrumentation and applications.* IEEE Rev Biomed Eng, 2013. **6**: p. 99-110.

103. Mitrou, N., et al., *Laser speckle contrast imaging reveals large-scale synchronization of cortical autoregulation dynamics influenced by nitric oxide.* Am J Physiol Renal Physiol, 2015. **308**(7): p. F661-70.

104. Scully, C.G., et al., *Segmentation of renal perfusion signals from laser speckle imaging into clusters with phase synchronized dynamics.* IEEE Trans Biomed Eng, 2014. **61**(7): p. 1989-97.

105. Newman, M.E., *Modularity and community structure in networks.* Proc Natl Acad Sci U S A, 2006. **103**(23): p. 8577-82.

106. Bryden, J., et al., *Stability in flux: community structure in dynamic networks.* J R Soc Interface, 2011. **8**(60): p. 1031-40.

107. Andreasen, F., et al., *The influence of age on renal and extrarenal effects of frusemide.* Br J Clin Pharmacol, 1984. **18**(1): p. 65-74.

108. Beutler, J.J., et al., *Comparative study of the effects of furosemide, ethacrynic acid and bumetanide on the lithium clearance and diluting segment reabsorption in humans.* J Pharmacol Exp Ther, 1992. **260**(2): p. 768-72.

109. Colussi, G., et al., *Effects of acute administration of acetazolamide and frusemide on lithium clearance in humans.* Nephrol Dial Transplant, 1989. **4**(8): p. 707-12.

110. Dupont, A.G., et al., *Renal pharmacodynamic effects of torasemide and furosemide in normal man.* Arzneimittelforschung, 1988. **38**(1A): p. 172-5.

111. Scherzer, P., H. Wald, and M.M. Popovtzer, *Enhanced glomerular filtration and Na+-K+-ATPase with furosemide administration.* Am J Physiol, 1987. **252**(5 Pt 2): p. F910-5.

112. Lauridsen, I.N., et al., *Abnormal glomerular and tubular response to intravenous frusemide in patients with chronic glomerulonephritis.* Nephrol Dial Transplant, 1991. **6**(7): p. 466-75.

113. Matthesen, S.K., et al., *Effect of amiloride and spironolactone on renal tubular function, ambulatory blood pressure, and pulse wave velocity in healthy participants in a double-blinded, randomized, placebo-controlled, crossover trial.* Clin Exp Hypertens, 2012. **34**(8): p. 588-600.

114. Freudenthaler, S., et al., *Do alterations of endogenous angiotensin II levels regulate erythropoietin production in humans?* Br J Clin Pharmacol, 2003. **56**(4): p. 378-87.

115. Johnston, G.D. and A.P. Passmore, *The effects of cilazapril alone and in combination with frusemide in healthy subjects.* Br J Clin Pharmacol, 1989. **27 Suppl 2**: p. 235S-242S.

116. Christensen, S. and J.S. Petersen, *Effects of furosemide on renal haemodynamics and proximal tubular sodium reabsorption in conscious rats.* Br J Pharmacol, 1988. **95**(2): p. 353-60.

117. Tucker, B.J. and R.C. Blantz, *Effect of furosemide administration on glomerular and tubular dynamics in the rat.* Kidney Int, 1984. **26**(2): p. 112-21.

118. Wang, X., et al., *Effects of inhibition of the Na+/K+/2Cl- cotransporter on myogenic and angiotensin II responses of the rat afferent arteriole.* Am J Physiol Renal Physiol, 2007. **292**(3): p. F999-F1006.

119. Miracle, C.M., et al., *Combined effects of carbonic anhydrase inhibitor and adenosine A1 receptor antagonist on hemodynamic and tubular function in the kidney.* Kidney Blood Press Res, 2007. **30**(6): p. 388-99.